Marine Micropaleontology 203 (2026) 102553

Contents lists available at ScienceDirect

Marine Micropaleontology

journal homepage: www.elsevier.com/locate/marmicro

Research paper

Marine benthic foraminifera diversity in extreme environments: A case study from the Edisto Bay (Ross Sea, Antarctica)

F. Caridi [a,*], L. Langone [b], A. Sartini [c,d], C. Morigi [d], G. Galli [c,d], P. Giordano [b], M. Bensi [e], V. Kovacevic [e], L. Ursella [e], N. Krauzig [a,f], A. Sabbatini [a]

[a] Department of Life and Environmental Sciences, Polytechnic University of Marche, 60122 Ancona, Italy
[b] Institute of Polar Sciences, National Research Council, Bologna, Italy
[c] Department of Environmental Sciences, Informatics and Statistics, University of Ca' Foscari Venice, 30172 Venice, Italy
[d] Department of Earth Sciences, University of Pisa, 56126 Pisa, Italy
[e] Institute of Oceanography and Experimental Geophysics-OGS, 34010 Trieste, Italy
[f] GEOMAR Helmholtz Centre for Ocean Research Kiel, 24148 Kiel, Germany

A B S T R A C T

Antarctica and its coastal systems are highly sensitive to climate change, with rapidly evolving environmental conditions affecting benthic ecosystems. This study presents a detailed analysis of living benthic foraminiferal communities in Edisto Inlet (Ross Sea, Antarctica), a poorly explored coastal area. We investigated the spatial distribution of foraminiferal assemblages and their relationship with environmental variables, including sedimentation rate, redox potential, organic matter content, and bottom currents. By integrating foraminiferal, sedimentological, and oceanographic data, three distinct environmental zones were identified within the inlet, revealing pronounced ecological gradients: outer (station 180), middle (station 24), and inner (station 34). The outer zone exhibited high-energy conditions, well-oxygenated sediments, and diverse, abundant communities dominated by calcareous species *Trifarina angulosa*, monothalamous morphotypes *Micrometula* sp., and agglutinated taxa (*Miliammina arenacea, Portatrochammina antarctica*). The middle section, characterized by moderate sedimentation and suboxic conditions, supported lower diversity and abundance, with agglutinated species (*Paratrochammina bartrami, Portatrochammina antarctica*) and monothalamous taxa (*Tinogullmia* sp., *Psammophaga magnetica*) thriving in organic-rich sediments. The inner zone presented low-energy, highly hydrated sediments with strong microbial activity, a markedly reduced redox potential, and suboxic to anoxic conditions, where opportunistic calcareous (*Globocassidulina biora, Globocassidulina subglobosa, Bolivinellina pseudopunctata*) and monothalamous species (*Psammosphaerid* spp., *Hippocrepinella hirudinea*) persisted. Overall, our findings emphasize the strong link between benthic foraminiferal assemblages and local physico-chemical conditions, providing essential ecological baselines for Antarctic fjord systems. By demonstrating the responsiveness of living foraminifera to environmental variability, this study offers valuable insights into present ecosystem functioning and the implications of ongoing climate change for polar coastal environments.

1. Introduction

Antarctica and the Southern Ocean play a crucial role in regulating Earth's atmospheric and oceanic systems, making them essential components of global climate dynamics. The Antarctic Circumpolar Current (ACC) drives global ocean circulation, redistributing heat, nutrients, and oxygen, and facilitating carbon dioxide uptake and deep-ocean sequestration (Sabine et al., 2004; Hauck et al., 2015; Rogers et al., 2020; Lombardi et al., 2021). Climate change has been a major external driver of the drastic transformations observed in Antarctica (Clem et al., 2020; Stammerjohn and Scambos, 2020). In particular, the West Antarctic Peninsula is widely known to be one of the fastest warming regions on Earth, with an increase in some regions of 1.09 °C per decade in winter and a total increase in mean annual air temperatures of around 2.8 °C over the last century (Vaughan et al., 2003; Turner et al., 2005; Bromwich et al., 2014, 2025; Turner et al., 2021). As ice sheets and glaciers continue to melt at an accelerating rate, the influx of freshwater into the ocean disrupts salinity levels, affects ocean currents, and triggers cascading impacts on marine ecosystems and global climate patterns.

Among the most sensitive marine organisms are foraminifera, an abundant group of single-celled eukaryotic organisms that live in all aquatic environments (Murray, 2006). Their large abundance, combined with sensitivity to the environmental conditions and long-term preservation in sediments, makes benthic foraminifera a widely used proxy to reconstruct paleoceanographic and paleoclimatic changes (Murray, 2001; Gooday, 2003; Gooday and Jorissen, 2012; Saraswat et al., 2017). In Antarctica, many studies have analysed living and fossil assemblages across sites such as Terra Nova Bay, the Larsen Ice Shelf, Admiralty Bay,

* Corresponding author.
E-mail address: f.caridi@staff.univpm.it (F. Caridi).

https://doi.org/10.1016/j.marmicro.2026.102553
Received 16 October 2025; Received in revised form 21 January 2026; Accepted 21 January 2026
Available online 22 January 2026

and the Ross Sea, revealing their paleoenvironmental significance (Violanti, 1996; Murray and Pudsey, 2004; Majewski et al., 2005; Majewski and Anderson, 2009; Majewski, 2010; Capotondi et al., 2018, Capotondi et al., 2020; Majewski et al., 2020; Galli et al., 2023). Although numerous studies have examined dead foraminiferal assemblages (thanatocoenosis) for reconstructing past environments, fewer and only recent works have focused on living communities (biocoenosis), which are crucial for understanding present-day ecosystem dynamics. This knowledge gap is particularly evident in certain Antarctic coastal environments, such as Edisto Inlet. Recent ecological approaches have emphasized the value of benthic foraminifera as indicators of environmental change, capable of recording ecosystem responses to both natural and anthropogenic disturbances (Murray, 2014). Their distribution reflects multiple environmental parameters—such as organic matter availability, pH, oxygen levels, and current dynamics (Lutze and Coulbourn, 1984; Altenbach, 1992; Alve and Bernhard, 1995; Gooday and Rathburn, 1999; Van der Zwaan et al., 1999; Ernst et al., 2002; Ernst and van der Zwaan, 2004; Ernst et al., 2005; Ernst et al., 2006). However, the controlling factors vary regionally. In Antarctica, for example, several studies have identified the main drivers of foraminiferal distribution as variations in water masses with depth, seasonal sea ice melt, bottom current activity, and levels of primary productivity (Anderson, 1975; Milam and Anderson, 1981; Massom and Stammerjohn, 2010; Majewski and Anderson, 2009; Capotondi et al., 2018). Furthermore, studies conducted in the Ross Sea have shown that the preservation of calcareous species is limited by the shallow depth of the Calcite Compensation Depth (CCD), a result of low temperatures and high salinities, which favor the solution of $CaCO_3$ and, possibly, high concentrations of CO_2 (Kennett, 1966; Anderson, 1975; Capotondi et al., 2018).

In this complex ecological framework, benthic foraminifera, including monothalamids, have emerged as key components of Antarctic benthic ecosystems. Monothalamous foraminifera, although often overlooked in paleoenvironmental studies due to their fragile tests and limited preservation in sediment records, are among the most abundant and ecologically diverse groups in soft-bottom polar habitats (Gooday et al., 2004; Majewski et al., 2007; Sabbatini et al., 2007). These single-chambered forms show high adaptability to environmental gradients such as organic matter availability, oxygen levels, and sediment texture, and often dominate in glacially influenced and high-latitude environments (Caridi et al., 2021; Sabbatini et al., 2023; Fossile, 2022). Some opportunistic monothalamous species are among the first to colonize disturbed sediments, providing insights into the recovery and dynamics of benthic communities following environmental stress or disturbance events (Pawlowski et al., 2008; Gooday and Jorissen, 2012). Their presence and distribution can thus provide valuable insights into present-day ecosystem functioning and the response of polar benthic organisms to environmental change. A comprehensive ecological approach that includes polythalamous calcareous, agglutinated, and monothalamous taxa not only allows a more detailed characterization of benthic foraminiferal community structure, diversity, and composition, but also enables the identification of key environmental drivers shaping these communities. By integrating species-specific responses with quantitative measures such as abundance and distribution patterns, ecological analyses can detect subtle environmental gradients and early signals of stress or disturbance that might not be captured by physical or geochemical measurements alone. This approach is particularly critical in poorly explored coastal Antarctic systems, where baseline ecological data are scarce, and the establishment of reference conditions is needed. Understanding how benthic foraminiferal communities respond to natural variability and anthropogenic pressures provides a framework for predicting future ecosystem changes and assessing ecosystem resilience. In this context, ecological analyses offer a robust and complementary tool for monitoring environmental change over time, informing conservation strategies, and supporting broader efforts to model polar marine ecosystems under climate-driven shifts.

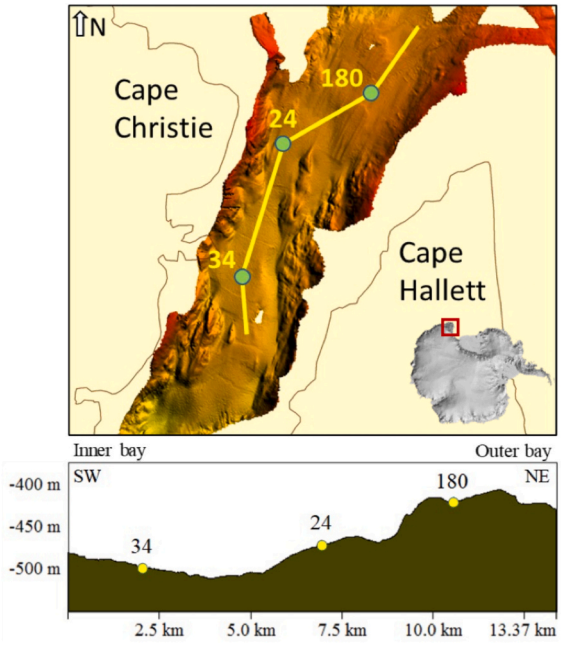

Fig. 1. Map and bathymetric reconstruction of the Edisto Inlet with the three sites (station 180, 24, 34), investigated in this work.

Therefore, the present work aims to study and characterize the assemblages of living benthic foraminifera located in the area of Edisto Inlet and analyze their response in relation to different environmental variables (sedimentation rate, temperature, pH, redox conditions (Eh), organic matter content, and bottom currents). In addition, this study will allow us to fill current knowledge gaps regarding the presence and distribution of benthic foraminifera in this area, a region of Western Antarctica that is still poorly studied from an ecological perspective.

2. Materials and methods

2.1. Area of study

Edisto Inlet is a small fjord located in the northern Victoria Land coast (Fig. 1), enclosed between the Hallett Peninsula and Cape Christie. It is 15 km long and 4 km wide, reaching a depth of about 600 m with a reverse slope with the shallower part pointing toward its entrance, where it reaches a depth of about 100 m and connects to the Moubray Bay (Battaglia et al., 2024). The area is characterized by distinctive oceanographic conditions and strong seasonality in sea-ice cover, which typically forms during the austral winter and reaches its maximum extent between August and October, with a minimum in February (Falco et al., 2024). Circulation within the fjord is influenced by a double-layer stratification at its entrance, with a thermocline/halocline/pycnocline between ~50 and 150 m depth, and by a gyre-like circulation pattern, with south–southwestward flow along the western flank and north–northeastward flow along the eastern flank (Battaglia et al., 2024).

At the broader Ross Sea continental shelf scale, ocean circulation is governed by the interaction between locally-formed dense shelf waters and intrusions of modified Circumpolar Deep Water (mCDW), which

Table 1
Sampling sites position and depth about the multicorer (MUC) sampled stations 180, 24, 34.

MUC Station	Latitude (°N)	Longitude (°E)	Depth (m)
180	−72.2941	170.1464	419
24	−72.3081	170.0560	475
34	−72.3485	170.0139	496

transports relatively warm and saline waters onto the shelf (Smith Jr et al., 2014; Castagno et al., 2017). These intrusions may play a secondary role in polynya formation, which, as is well known, is primarily controlled by atmospheric forcing, coastal geometry, and sea-ice dynamics. Furthermore, continuous ice production within these polynyas leads to strong surface cooling and brine rejection, driving the formation of High Salinity Shelf Water (HSSW), a key precursor of Antarctic Bottom Water (AABW)(Orsi and Wiederwohl, 2009; Kohut et al., 2013; Xu et al., 2021; Xie et al., 2025). The inflow of nutrient-rich mCDW onto the shelf promotes high primary productivity, sustaining local marine ecosystems, while HSSW and AABW play a key role in the global thermohaline circulation, deep ventilation, and climate regulation (Orsi et al., 1999; Johnson, 2008; Silvano et al., 2023; Ainley et al., 2024).

2.2. Sample acquisition and storage

Sediment samples for this study were collected between 9 and 14 February 2023 on board the R/V *Laura Bassi*, during Leg 2 of the PNRA XXXVIII Antarctic Expedition, as part of the LASAGNE project. Undisturbed surface sediments were retrieved from three sites (stations 180, 24, and 34_Fig. 1 Table 1) using an Oktopus MC08–12″ series multicorer (12 tubes, Ø 100 mm × 610 mm). At each site, eight replicate cores (MUCs) were collected for different analytical purposes. Specifically, for the present study, two cores (R1 and R2) from each site were analysed for living benthic foraminiferal assemblages, one core (R3) was used for pH and redox potential measurements, and one core (R4) for magnetic susceptibility analysis. The sediment cores, not processed on board, were stored at +4 °C in an ISO20 refrigerated container and transported to Italy for subsequent specific analyses.

2.3. Thermohaline properties and ocean current data

Hydrographic CTD (conductivity-temperature-depth) vertical profiles (reaching maximum depths of about 4–6 m above the sea floor) were recorded at 61 stations with a Seabird SBE 911plus, equipped with additional sensors for dissolved oxygen, fluorescence, and turbidity. Data were collected both at the entrance of the Edisto Inlet, which was still partially covered by seasonal sea ice (the sea ice opening of the inlet is highly variable), and in the interior of the inlet.

Two lowered L-ADCPs (Workhorse I Teledyne RD Instrument, 300 kHz, up and down looking) were deployed together with the CTD-Rosette system at each CTD station. A total of 58 L-ADCP profiles were recorded with vertical bins every 5 m.

CTD raw data were converted, processed, and quality controlled using the SBE Data Processing software and MATLAB routines (The MathWorks Inc., 2024). Derived variables (i.e., potential temperature θ with reference to 0 dbar, practical salinity S, potential and neutral density) were calculated from *insitu* data using the Ocean Data View (ODV; Schlitzer, 2025) with the toolbox TEOS-10 (Gibbs SeaWater Oceanographic Toolbox, www.teos-10.org/software.html). Dissolved Oxygen concentration was measured using an SBE43 sensor. T and S data were quality controlled and averaged every 1 dbar, with overall accuracy within ±0.002 °C for T, ± 0.005 for S, and 2% of saturation for oxygen. Fluorescence and turbidity in the water column were measured with optical sensors WET Labs ECO-AFL/FL.

2.4. Parameters of sediment samples

At each site, pH and redox potential (Eh) were determined using pre-calibrated Metrohm punch-in electrodes. Measurements were carried out on board immediately after recovery, with a centimetric vertical resolution. Magnetic susceptibility (MS, SI × 10^{-6}) was measured on replicate core R4 using an MS2F Surface Point Probe (Bartington Instruments Ltd., UK), with a vertical resolution of 1 cm. In the laboratory, sediment cores were split lengthwise into two halves. One-half was subsampled at 1 cm intervals, and each slice was split into several aliquots for measurements of water content, biogeochemical, and stable isotope analyses. The other half was photographed and X-rayed to identify subtle sedimentary structures, variations in density and texture, and signs of bioturbation, and was subsequently stored at 4 °C. Porosity (Φ) and water content (%) were calculated by measuring the weight loss of sediments dried overnight at 55 °C to constant weight, and assuming a particle density of 2.5 g cm^{-3} following Covelli et al. (2012). An aliquot of the freeze-dried and agate-mortar powdered sample was acidified with 1.5 M HCl, and subsequently analysed using a Thermo Fisher Elemental Analyzer (FLASH 2000 CHNS/O) coupled with a Thermo Fisher Scientific Delta Q isotope ratio mass spectrometer (IRMS) to determine organic carbon (OC, wt%), total nitrogen (TN, wt%), and stable carbon isotopes ($\delta^{13}C$, ‰) (Tesi et al., 2012). The sediment accumulation rates (SARs, cm $year^{-1}$) were calculated based on a Constant Flux: Constant Sedimentation (CF:CS) model applied on activity measurements of the short-lived radionuclide ^{210}Pb (half-time, 22.3 years). The ^{210}Pb analyses were carried out by alpha counting of its daughter isotope ^{210}Po, using a silicon barrier detector coupled with a multichannel analyzer. ^{210}Po was assumed to be in secular equilibrium with its grandparent ^{226}Ra, following the procedure described in Frignani et al. (2005).

2.5. Sample preparation for foraminiferal analysis

Two core replicates were analysed for each site for living foraminiferal assemblages. On board, each core was vertically split into two halves: one half was used for foraminifera analysis, while the other half was used for storage of other types of analyses. The half used for foraminiferal studies was then horizontally sectioned onboard: every 0.5 cm down to 2 cm depth, and then in 1 cm intervals down to 5 cm. The sediment core collected samples have then been treated with Cell Tracker Green CMFDA (CTG). CellTracker Green (CMFDA) is a molecule that uses fluorescent probes to label living cells as it can permeate freely through cell membranes (Bernhard et al., 2006; Pucci et al., 2009). Once inside, it remains trapped due to an enzymatic reaction that makes the compound unable to pass through membranes again. This process results in a permanent cell marking, allowing these cells to emit a bright green fluorescence when hit by a source of light at right wavelength (between 492 and 517 nm). The CTG labelled samples were then stored at 4 °C after being fixed in a diluted 4% formalin solution buffered with sodium tetraborate.

In the laboratory, sediment samples were washed with a 125 μm sieve, and the residue was observed with a Leica M205 FCA stereomicroscope, equipped with a specific set of fluorescence light filters (Plates I, II, and III). Each stained foraminifera was picked, counted, and sorted manually using a brush. Only specimens with at least one or more chambers with a notable degree of fluorescence were considered alive. Fragments from agglutinated species, such as *Reophax* sp., *Textularia* sp., and damaged individuals, were included in the total count only if they displayed sufficient fluorescence intensity; otherwise, they were omitted. Species identification was conducted at the morphological level. For hard test foraminifera, the taxonomy was based on reference works by Mackensen et al. (1990), Igarashi et al. (2001), Gaździcki and Majewski (2003), Majewski (2013) and Galli et al. (2023). For monothalamids, morphological identification followed the guidelines of Pawlowski and Majewski (2011), Caridi et al. (2023), and Sabbatini et al. (2004), among others used as references.

Quantitative data from all samples were standardized per 50 cm^3 of sediment to calculate densities and relative abundances. The data obtained from the two core replicates were averaged to obtain statistically representative values for each site. Furthermore, both densities and relative abundances have been evaluated in terms of vertical distribution and taxonomic composition in the sediment. In addition, species were classified in groups based on test material (Agglutinated, Calcareous, Organic) to assess potential adaptive advantages in different environmental settings.

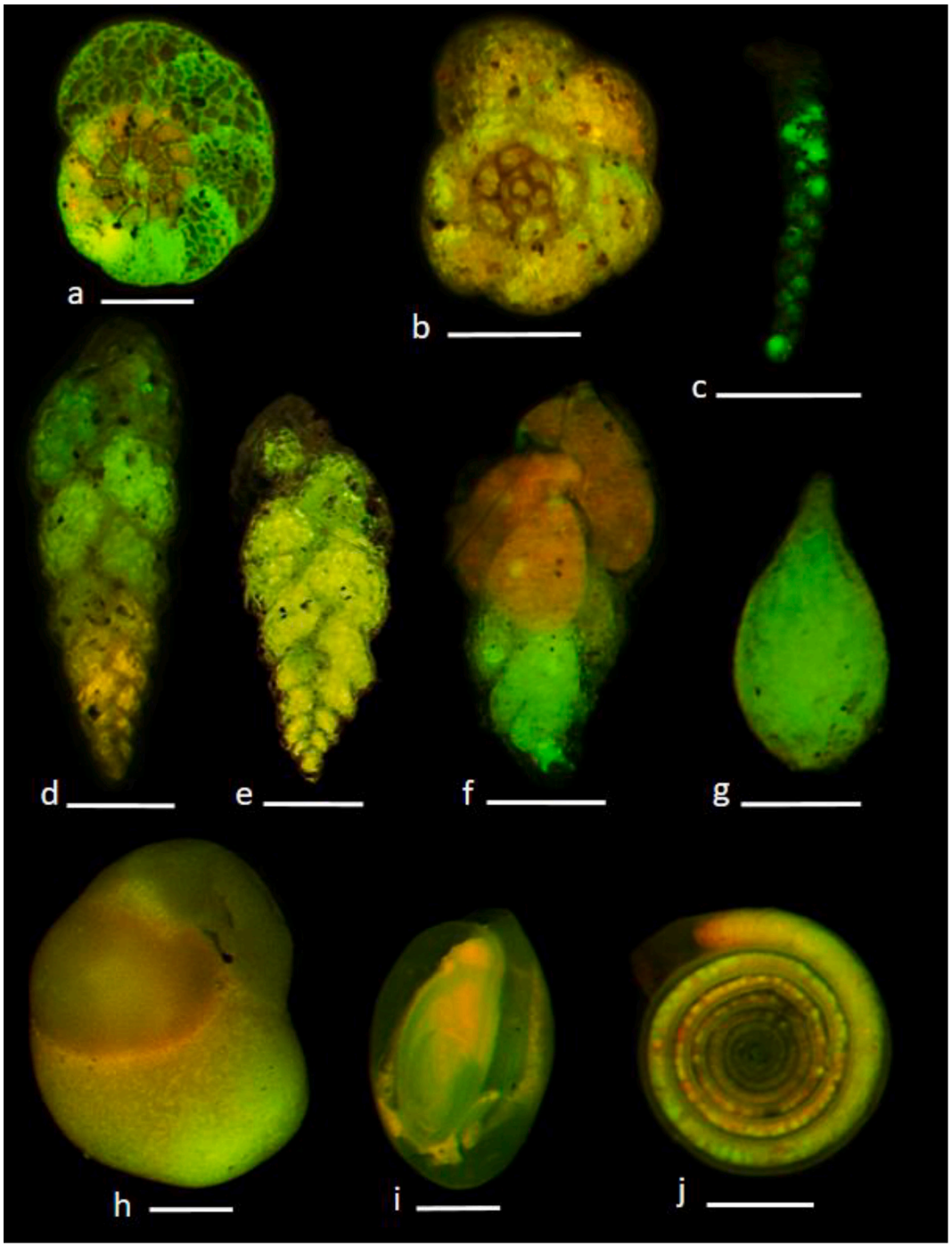

Plate I. Epifluorescence microscopy photos of (a) *Paratrochammina bartrami*, (b) *Portatrochammina antarctica*, (c) *Textularia earlandi*, (d, e) *Pseudobolivina antarctica*, (f) *Trifarina angulosa*, (g) *Nodosaria* sp., (h) *Globocassidulina biora*, (i) *Quinqueloculina seminula,* and (j) *Cornuspira planorbis*. Scale bar = 100 μm.

Overall densities (number of individuals/50 cm^3) of each station were converted into relative abundance for each species, highlighting all taxa with a relative abundance of at least 3% considering individuals from the whole samples. The remaining species that did not reach the 3% threshold fall under the "Total others" category.

The specific fraction corresponding to the 2–3 cm depth of the Station 180 R2 sediment core could not be analysed due to problems encountered during the sampling procedure.

2.6. Statistical data processing

Biodiversity indices (Simpson's Index, Pielou's Index) were calculated using PAST v4.17 (PAleontological STatistics; Hammer et al., 2001). Multivariate analyses were performed using the software R (R Core Team, 2024), including Analysis of Similarities (ANOSIM; Somerfield et al., 2021) to assess differences between or within sample groups, Non-metric Multidimensional Scaling (NMDS; Clarke and Ainsworth, 1993) to visualize dissimilarities among samples, and cluster analysis to group samples based on similarity.

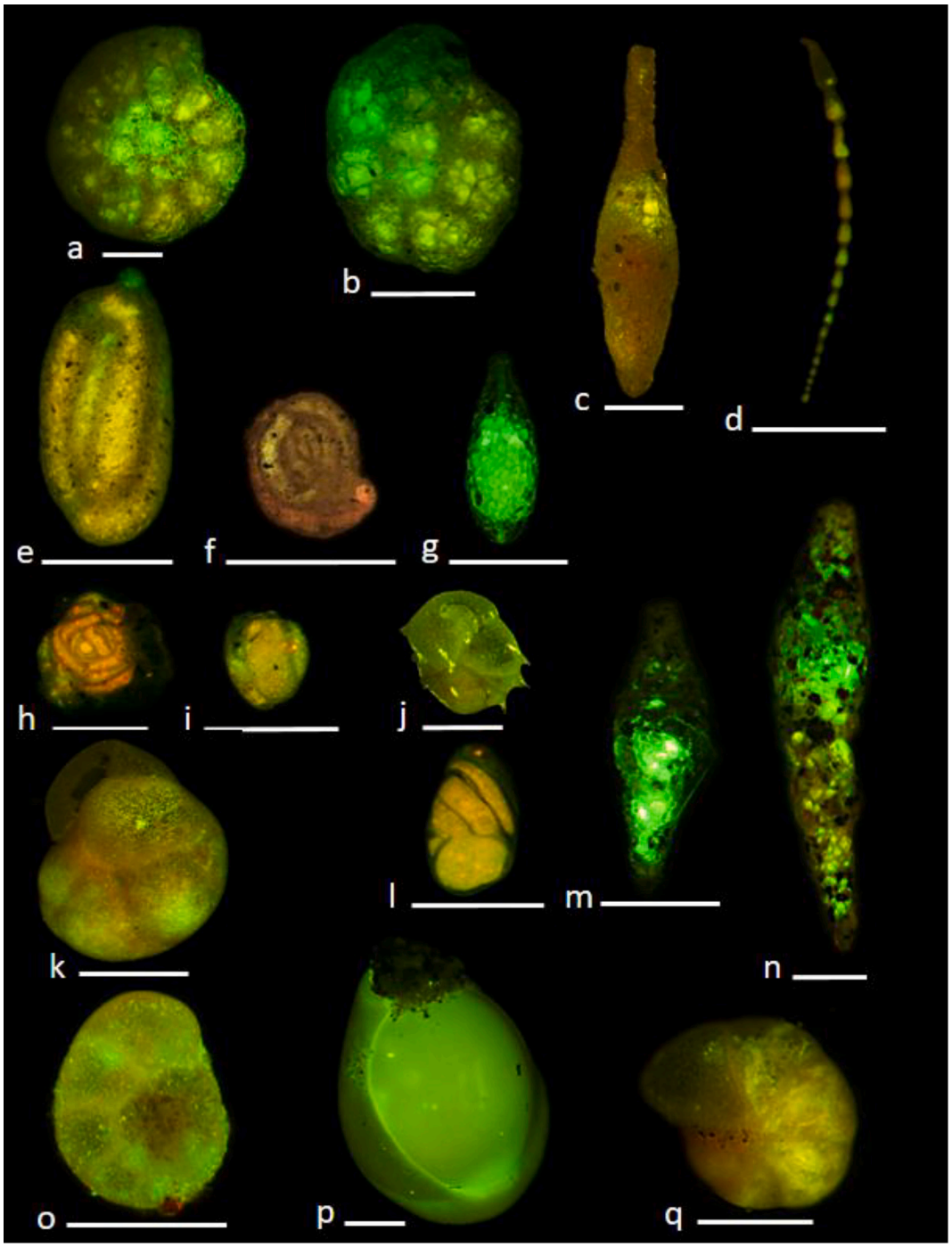

Plate II. Epifluorescence microscopy photos of (a) *Recurvoides turbinatus*, (b) *Recurvoides contortus*, (c) *Hormosinella ovicula* fragment, (d) *Leptohalysis scottii*, (e) *Miliammina arenacea*, (f) *Glomospira charoides*, (g) *Lagenammina difflugiformis*, (h) Ammovertellina sp., (i) *Adercotryma glomeratum*, (j) *Ehrenbergina glabra*, (k) *Globocassidulina subglobosa*, (l) *Robertina artica*, (m) *Reophax subfusiformis*, (n) *Nodulina dentaliniformis*, (o) *Rosalina globularis*, (p) *Pyrgo oblonga*, and (q) *Melonis affinis*. Scale bar = 250 μm.

3. Results

3.1. Thermohaline properties

An overview of the thermohaline structure based on data collected in February 2023 is compared with several profiles collected in the same month in 2020 and 2022 (Fig. 2). The water column within the bay remains largely stratified during austral summer, primarily due to the influence of relatively low-salinity surface waters resulting from seasonal sea ice melting, and to a greater influence of offshore waters, whose entry into Edisto is facilitated by reduced sea ice coverage. The stratification of the water column is further reinforced by the distinct characteristics of the inlet waters, which differ from the main Ross Sea water masses (Antarctic Surface Water, AASW, and Modified Circumpolar Deep Water, MCDW), with only some properties of Modified Shelf Water observed.

Surface layer conditions may vary interannually, likely in response to changes in sea ice extent and melting patterns, as suggested by profiles collected in 2020 and 2022 (Fig. 2). Complete mixing and homogenisation of the entire water column occur during the austral winter season

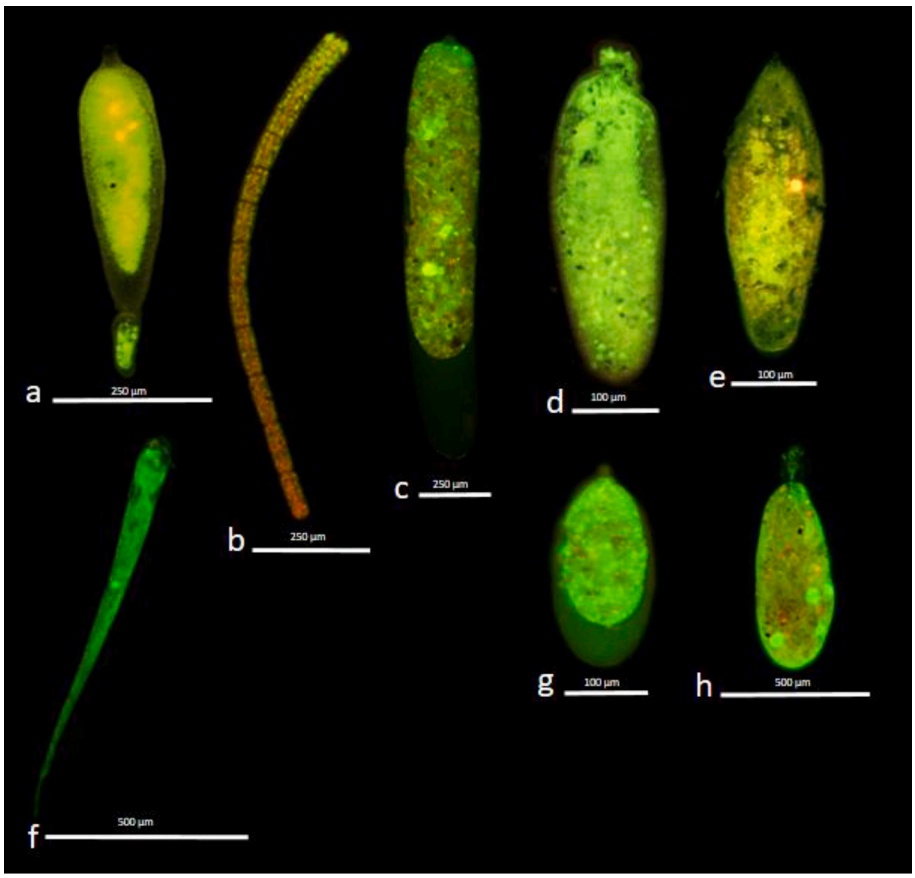

Plate III. Epifluorescence microscopy photos of (a) *Conqueria*-like sp., (b) *Nodellum*-like sp., (c) Elongated gromia, (d) *Phainogullmia aurata*, (e) *Psammophaga magnetica*, (f) *Micrometula* sp., (g) Oval gromia, and (h) *Vellaria*-like sp..

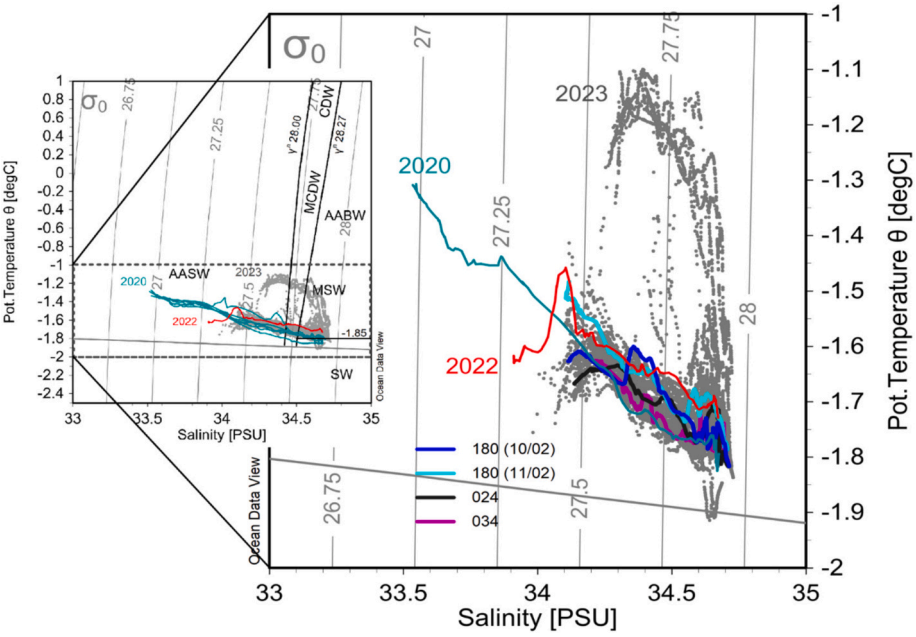

Fig. 2. Potential temperature θ - salinity scatter plot (with potential density anomaly σ_o referred to 0 dbar), expanded from the dashed rectangular area in the insert, indicates thermohaline structure in the Edisto Bay: grey dots are data collected in 2023, evidencing four CTD casts at three sampled stations 180, 024, and 034; red line is the unique profile recorded in 2022, bluish-green is one of the six stations in 2020. Insert plot: all available data from 2020 (six CTD casts), 2022 (1 CTD cast), and 2023 (61 CTD casts) compared to typical principal water masses of the Ross Sea: AASW Antarctic Surface Water, MCDW Modified Circumpolar Deep water, AABW Antarctic Bottom Water, SW Shelf Water, and MSW Modified Shelf Water, according to Orsi et al. (1999). The black line is potential temperature − 1.85 °C, and black curves are neutral density of 28.00 kg m^{-3} and 28.27 kg m^{-3} adapted from Orsi et al. (1999), to delimit the Ross Sea water masses. A grey solid line in both plots is a surface freezing point. (For interpretation of the references to colour in this figure legend, the reader is referred to the web version of this article.)

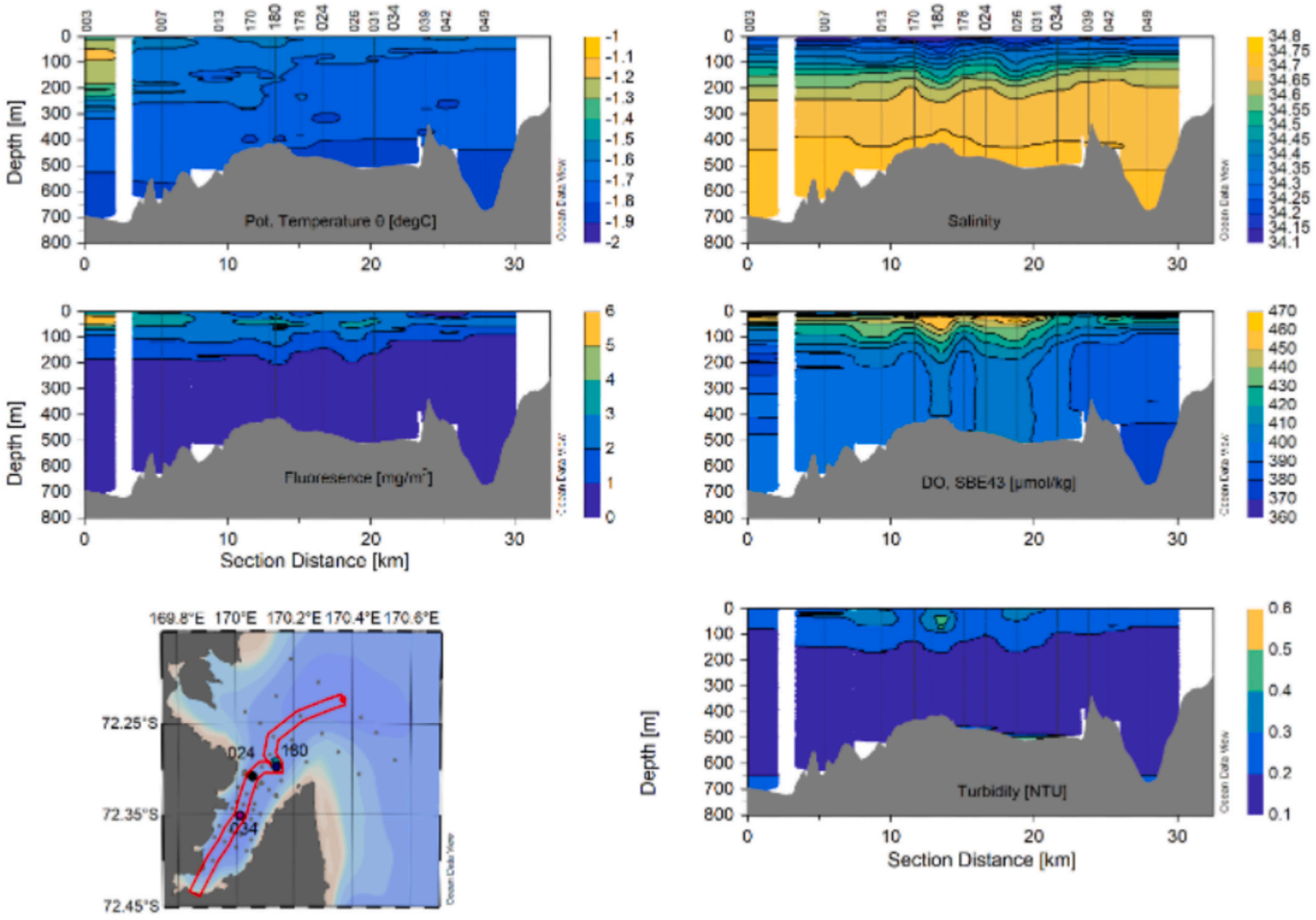

Fig. 3. Transect extending from the outer to the inner sector of Edisto Bay, encompassing sampled stations 180, 24, and 34: vertical section of the potential temperature, salinity, fluorescence, dissolved oxygen and turbidity in February 2023.

(from July to November), as evidenced by oceanographic mooring data at the entrance to Edisto Bay (Langone and The LASAGNE Team, 2024).

The vertical sections of thermohaline properties along the transect extending in the alongshore direction from the outer to the inner sector of the bay, and including all three sampled stations investigated in this study (Fig. 3), show a highly stratified upper layer. A halocline (corresponding to the pycnocline, see Fig. 4, protrudes to the depth of around 250 m, below which the water is much more uniform, and properties are relatively constant. The uppermost stratified layer is relatively thin at the head of the bay, and gradually widens, and deepens toward the mouth, as the mixing with the surrounding waters takes place.

The specific physio-chemical parameters of the water column for the three sampled stations (Fig. 4) are based on four CTD profiles. Two of these profiles were collected near station 180 on different dates. All four profiles exhibit similar trends in the physical parameters. In general, temperature slightly decreases from the surface to the bottom, while salinity and density increase. Below 250 m depth, salinity and density become more uniform, with low vertical gradients.

Oxygen concentration shows a minimum near the surface, corresponding to the low-salinity waters influenced by sea ice melt. Maximum oxygen values are observed at around 50 m depth, after which concentrations gradually decrease and remain relatively uniform from 250 m to the bottom. These measurements indicate the presence of a two-layer stratification: the upper layer, extending to approximately 250 m, is characterized by variable temperature and salinity, while the deeper layer (>250 m) displays more uniform thermohaline properties and dissolved oxygen concentrations (Fig. 4). Simultaneously, fluorescence and turbidity in the water column (from the CTD sensors) reach maximum values in the upper layer, and only turbidity slightly increases in the deep layers at stations 24 and 34. In addition, the first turbidity profile acquired at station 180 (dark blue line) presents a peak in the layer 0–100 m, which disappears approximately 22 h later (light blue line). Horizontal current profiles gathered during CTD casts reveal marked temporal and vertical variability (Fig. 4). At station 180, the maximum current speed reaches 0.21 m/s at 75 m depth on the first day of measurements. Current velocities are highest in the upper layer (0.13–0.19 m/s), decrease markedly between 200 and 300 m (with a local increase to ~0.10 m/s near 200 m), and range between 0.12 and 0.13 m/s in the deepest layer. The repeated profile shows an overall reduction in velocity as well as a reduction in turbidity in the upper layer. A maximum speed is 0.11 m/s at 120 m depth, minimum is 0.02 m/s, and near-bottom speed is 0.03 m/s. Local maxima and minima occur out of phase with the previous profile — where the current is strongest in the first cast, it weakens in the second, and vice versa — further supporting the influence of short-term tidal variability. Near-bottom current speeds are larger (0.13 m/s) during the first and smaller (0.03 m/s) during the second measurement.

At stations 22 and 34, current profiles also exhibit vertical variability, although maximum velocities do not exceed ~0.10 m/s. In all three locations, current speed does not vary uniformly with depth and occasionally retains elevated values within the deep layers, suggesting the influence of localized circulation cells or bottom-intensified flow.

These variations indicate that hydrodynamic conditions in the fjord are influenced not only by thermohaline gradients but also by short-term processes such as tidal forcing and inertial oscillations. Current velocity and direction (not shown) vary throughout the water column, from the

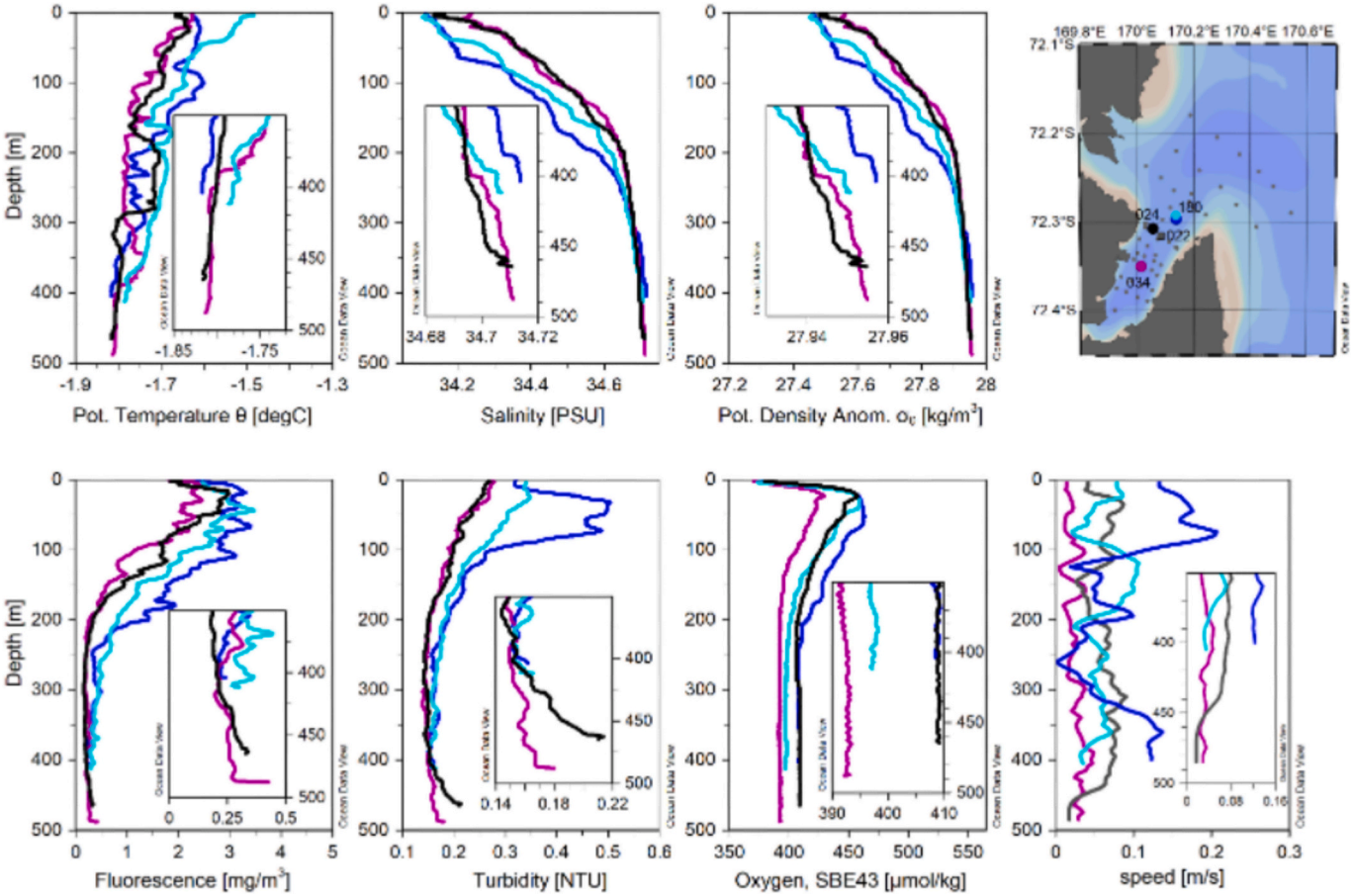

Fig. 4. Complete vertical profiles and zoom into the deepest layer (350–500 m depth) at stations 180, 24, and 34 collected in February 2023: potential temperature, salinity, potential density anomaly, fluorescence, turbidity, dissolved oxygen, and current speed from CTD and L-ADCP data. The inset map shows the locations of the sampled stations. L-ADCP horizontal currents at station 22 are shown in place of the missing profile at station 24. Sampling times (UTC): station 180 on 10 February, around 10 am/ 11 February, around 8 am (dark/light blue lines), station 24 on 10 February at around 02 am, station 34 on 13 February at around 09 am, and station 22 (for currents only) on 12 February at around 10 pm. (For interpretation of the references to colour in this figure legend, the reader is referred to the web version of this article.)

surface to the seafloor, and considerable speeds (> 0.10 m/s) occur in the deep layer, not only near the surface. Here, we report only instantaneous speeds at the time of sampling because the current flow periodically changes direction, mainly due to baroclinic tidal variability (with periods of about 24 and 12 h). For example, at station 180, in the upper 100 m the flow is directed southward; between 100 and 200 m it is mainly in the *E*-W direction; and in the deep layer between 300 and 400 m, it is again southward, with varying speed as shown in the profile (Fig. 4). The currents at station 22 are directed opposite to those at station 180, but direct comparison is not possible because speeds and directions vary with tidal phase, and the measurements are not simultaneous.

3.2. Geochemical and physical parameters

Geochemical and physical profiles for the three studied stations reveal pronounced spatial gradients in sedimentation patterns, redox conditions, and organic matter (OM) content and preservation (Fig. 5).

SAR varies significantly within the Edisto Inlet, with low values calculated at the outer station 180 (0.073 cm/y), and a higher rate at the mid fjord station 24 (0.169 cm/y). The ^{210}Pb activity–depth profile of core from the innermost basin (station 34) does not permit a reliable estimation of the sediment accumulation rate, most likely due to a very high particle flux.

MS is highest at the outer station (average MS = 583 at station 180), decreasing progressively toward the inner station (average MS = 65 at station 24, and average MS = 7 at station 34). Porosity values are lower at the outer station 180 (average F = 0.53, 31% water content), where recent sediments are dominated by a massive, dark olive-grey (Munsell chart 5y 3/2), silty-sand component. Evidence of bioturbation is visible within the first 4 cm. In contrast, porosity remains consistently high in the two cores inside the fiord (average F = 0.85, 73% water content in station24, and average Φ = 0.96, 91% water content in station34). The inner stations are characterized by highly hydrated, fine-grained biogenic sediment. At Station 24, the recent sediments consist of alternating patches of olive-colored mud (Munsell chart 5Y 4/3) and very dark grey mud (Munsell chart 5Y 3/1), likely reflecting variations in the diatom ooze content. At station 34, surficial sediments (upper 1 cm) are olive colored (Munsell chart 5y 4/3), while deeper layers are uniformly black colored (Munsell chart 5y 2.5/1), and emitted a strong hydrogen sulfide odor. No sedimentary structures are visible in the upper-recent sediment layers of the three stations, as confirmed by both photography and x-ray profiles imaging (Fig. 5).

Eh values in the surface sediments are generally positive to slightly negative within the surficial 5 cm at station 180 and station 24 (average values of −30 mV and 8 mV, respectively), with the most positive values recorded at the sediment–water interface at station 180 (lev. 0–1, 228 mV). In contrast, Eh values at station 34 are strongly negative, with extremely low values already recorded in the surface sediments (−422 mV). This redox state remains essentially unchanged with increasing sediment depth (average Eh = −449 mV), indicating strongly anoxic conditions. The pH values at station 180 remain nearly constant

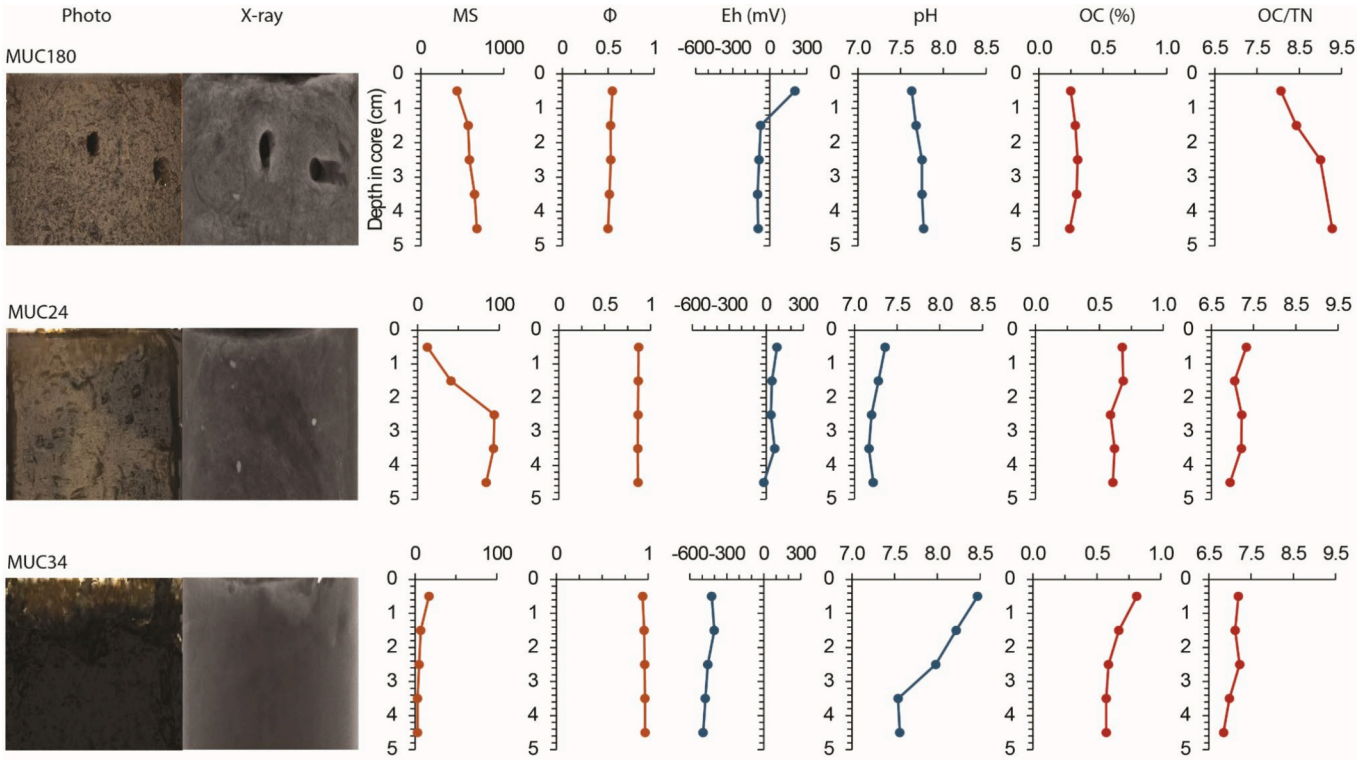

Fig. 5. Biogeochemical parameters and physio-chemical measurements in the first 5 cm of sediments at the three stations. MS: magnetic susceptibility, Φ: Porosity; OC=Organic Carbon (%), C/T = organic carbon vs total nitrogen molar ratio.

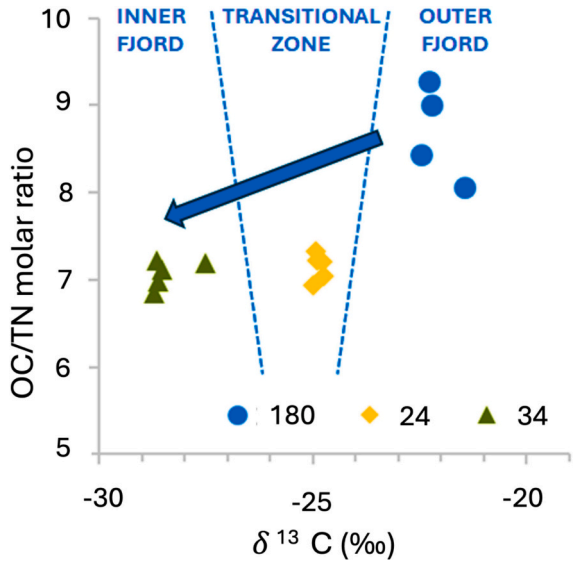

Fig. 6. Depositional settings and OM degradation pathways. $\delta^{13}C$ and C/N ranges for organic inputs along the Edisto Inlet, identifying three distinct zones: (i) an **outer fjord** zone, high energy, oxygenated reworking of low-reactivity sediments, dominated by low fresh marine inputs and low diagenetic alteration; (ii) a **transitional** mid-fjord **zone** influenced by both marine production and early diagenetic processing; and (iii) an **inner fjord** zone, low-energy and anoxic zone where OM is more isotopically depleted and degradation is slowed by persistent reducing conditions. Top-bottom red arrow corresponds to decreasing C/N values with increasing sediment depth; blue arrow indicates decreasing burial efficiency toward the inner fjord. (For interpretation of the references to colour in this figure legend, the reader is referred to the web version of this article.)

throughout the core (pH = 7.6 to 7.8), while at station 24, a slight decrease in pH with sediment depth is observed (pH = 7.5 to 7.3). A different situation is observed at station 34, where the pH reaches weakly alkaline values (7.5–8.5) within the upper 4 cm of sediment, before decreasing below that depth. OC content in sediments is generally low throughout the study area. At station 180, OC concentrations are lower (average OC = 0.3%), with relatively high C/N ratios (8.7). In contrast, surface sediments at station 24 show higher OC content (0.68%), which slightly decreased with sediment depth. C/N ratios are lower and decreased with depth (from 7.3 to 6.9). Station 34 exhibits the highest OC concentration in surface sediments (0.81%), with a sharp decline at depth (down to 0.57%). C/N ratios start around 7.2 at the surface and slightly decrease with depth to 6.8. The C/N ratio ranges from ~7 to >9 across the sites, with the highest values in the deeper layers of station 34 and station 180 (Fig. 5).

The $\delta^{13}C$ and C/N molar ratio data from the three stations along the Edisto Inlet fjord reveal a clear spatial pattern that reflects the origin, composition, and diagenetic state of sedimentary organic matter (OM), identifying three distinct zones characterized by different depositional settings and OM degradation pathways (Fig. 6). At the outer fjord zone, represented by station 180, $\delta^{13}C$ values range from −21 to −23‰ with relatively high C/N ratios (8.1–9.3) (Meyers, 1997; Lamb et al., 2006). At the transitional zone, represented by station 24, $\delta^{13}C$ values are more depleted (−24.5 to −25‰), and C/N ratios are slightly lower (~7.14). The inner fjord zone, represented by station 34, shows the most depleted $\delta^{13}C$ values (−27.5 to −28.5‰) and C/N values also below 7.

3.3. Benthic foraminiferal fauna

A total of 2646 living individuals were found across all the samples from all three stations; 63 different taxa were identified on the basis of morphological features at the species level, when possible. Community structures were evaluated based on different characteristics such as density along sediment depth, taxonomic composition, morphology, and biodiversity.

Densities of benthic foraminiferal fauna in station 180 reach the

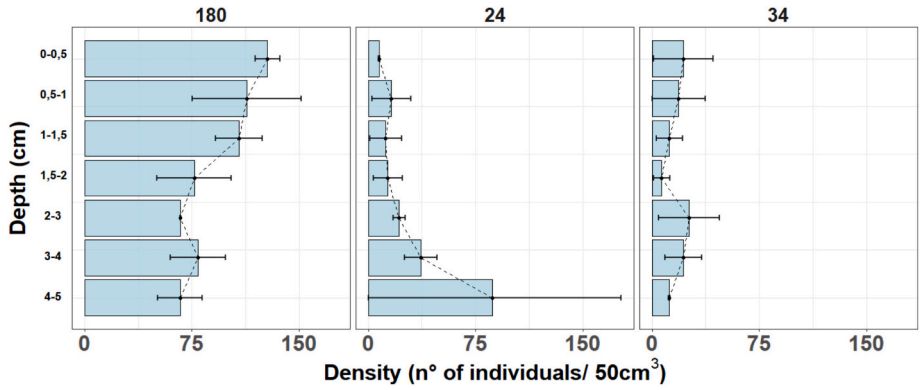

Fig. 7. Benthic foraminiferal density distribution in relation to the first 5 cm of the sediment, respectively from stations 180, 24, and 34.

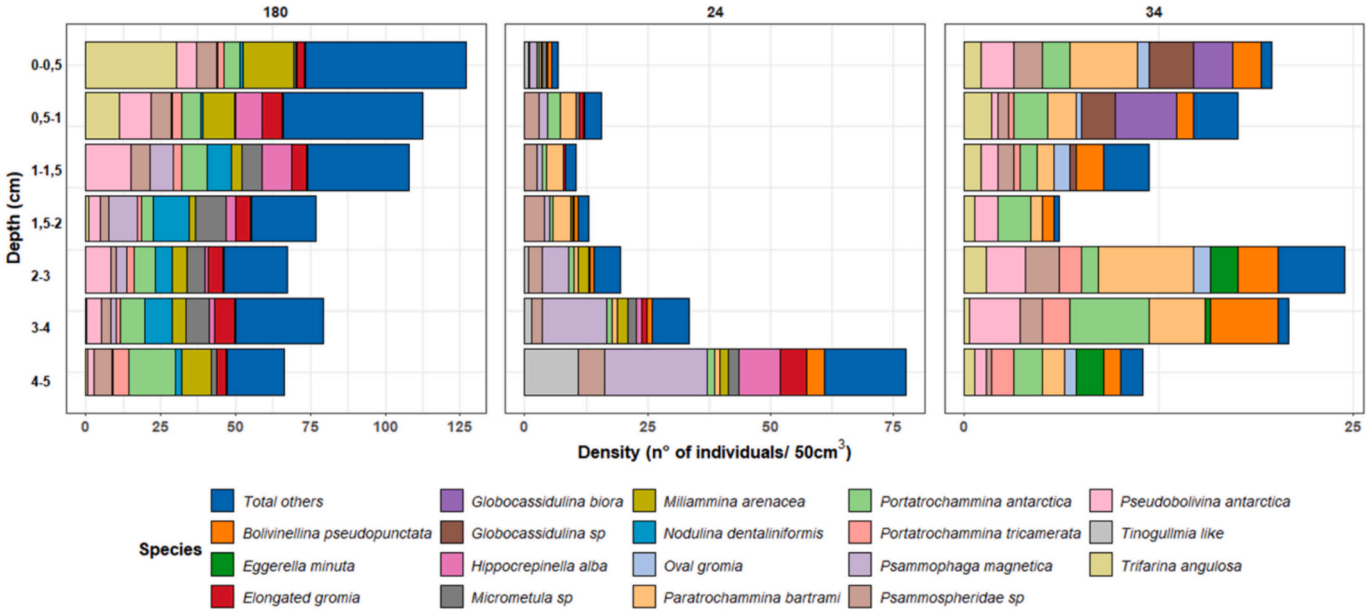

Fig. 8. Vertical distribution for each species that resulted in at least 3% of the total amount for each station.

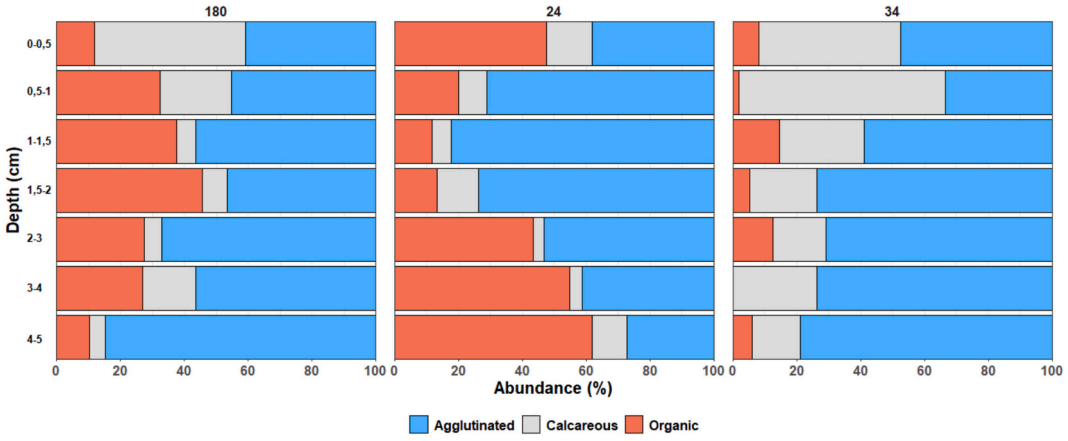

Fig. 9. Relative abundance of foraminiferal assemblages in the upper 5 cm of sediment cores from the three investigated stations, classified according to test composition.

highest values out of all three stations, with 128 individuals/50 cm^3 at the surface level (0–0.5 cm), showing a constant negative trend down-core, reaching 67 individuals/50 cm^3 at 4–5 cm (Fig. 7). Instead, station 24 is characterized by lower amounts of individuals in the upper 0–0.5 cm (8 individuals/50 cm^3), with higher densities at the deepest levels (4–5 cm; 87 individuals/50 cm^3). Station 34 has the overall lowest densities across all depths, moving from 22 individuals/50 cm^3 at the surface level (0–0.5 cm) to 12 individuals/50 cm^3 at 4–5 cm.

Vertical distribution of the most abundant species (≥ 3%) across the investigated stations is shown in Fig. 8. At station 180, the most abundant species is *Portatrochammina antarctica*, accounting for 8.7% of the total abundance, followed by *Miliammina arenacea* (8.3%), *Pseudobolivina antarctica* (8.2%), *Trifarina angulosa* (6.9%), *Nodulina dentaliniformis* (6%), and *Paratrochammina tricamerata* (3%). Among monothalamous taxa like elongated allogromiids (5.4%), *Psammospheridae* sp. (5.1%), and *Micrometula* sp. (5.3%) are also present.

In addition, *Portatrochammina antarctica* is present in sediments from station 34 where it accounts for 13.5% of the total assemblage. An even higher proportion is represented by another agglutinated species, *Paratrochammina bartrami*, which reached its highest relative abundance (17%) at station 34. *Pseudobolivina antarctica,* another agglutinated species, is also present and accounts for 10.3% of the total. Among the calcareous species, *Bolivinellina pseudopunctata* (12%), *Trifarina angulosa* (6.4%), and *Globocassidulina biora* (5.8%) are the most abundant. In station 24, apart from two species *P. bartrami* (7.2%) and *Portatrochammina antarctica* (6.9%), soft-shelled taxa largely dominated the assemblage. *Psammophaga magnetica* is the dominant species accounting for 23.6% of the total abundance, followed by *Psammospheridae* sp. (10.7%), *Tinogullmia*-like (7.2%) and *Hippocrepinella alba* (5%).

Benthic foraminiferal communities at three sites are generally dominated by agglutinated species (Fig. 9). At station 34, agglutinated species are less than 58% of the total benthic foraminiferal composition below 1 cm depth. Agglutinated species comprise an average of 40% at station 180, with a peak at 4–5 cm depth (85%). Station 24 differs from the other because of the increasing abundance of monothalamids, which exceeded 40% below 2 cm depth. Calcareous species also represent a significant portion of the community, especially at station 180 (47% at 0–0.5 cm depth) and station 34 (64% at 0.5–1 cm depth) (Fig. 9).

3.4. Biodiversity indices and multivariate analysis

The highest number of individuals (standardized per 50 cm^3) can be found in station 180, counting up to 637 individuals and 51 different species, followed by station 24 (193 individuals, 29 species) and station 34 (115 individuals, 23 species) (Table 2). Dominance (D) values are overall low, values results <0.1 in all three sites. This is also confirmed by Simpson's Index (D′), resulting in relatively high values in all sites, with station 180 being the highest (D′ = 0.9541). Evenness index (e^H/S) increases progressively moving from station 180 (e^H/S = 0.5696) toward station 24 (e^H/S = 0.6252) and station 34 (e^H/S = 0.7106), meaning that the species tend to be more clustered in station 180, while they are more evenly spread in different layers of sediment in station 24 and station 34.

The analysis of similarities (ANOSIM; Fig. 10) confirms strong differences in taxonomic composition among the stations (R = 0.72, p < 0.001), indicating that dissimilarity between stations is greater than within each station. Notably, station 24 exhibits the highest internal variability, whereas stations 180 and 34 show lower internal variability.

The NMDS plot (Fig. 11) shows a clear separation between station 180 and station 34, indicating that the samples from the two stations are very different, while station 180 and station 24 partially overlap, suggesting some affinities among the samples. The stress value of 0.16 denotes that the NMDS analysis is fitted well enough to illustrate the dissimilarities among the sites investigated in this research.

Table 2
List of the principal biodiversity parameters and indices evaluated in this work.

	180	24	34
Taxa Species	51	29	23
Individuals	637	193	115
Dominance D	0.4587	0.08797	0.07963
Simpson (D′)	0.9541	0.912	0.9204
Evenness (e^H/S)	0.5696	0.6252	0.7106

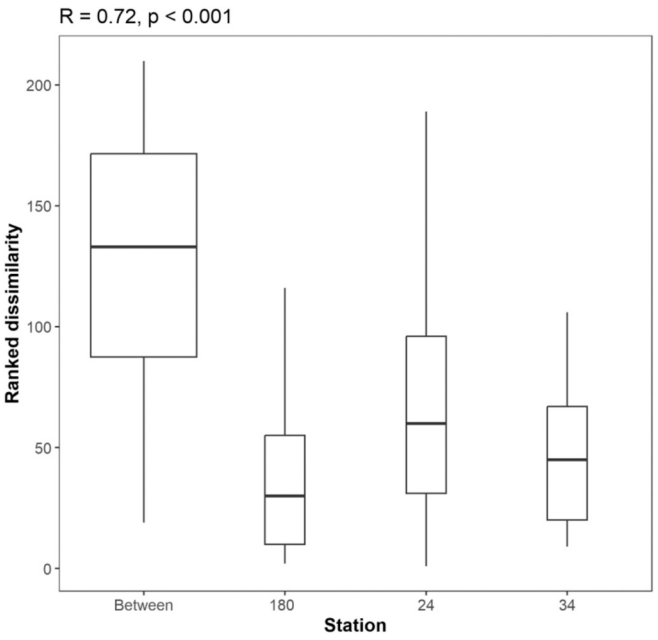

Fig. 10. Analysis of similarities (ANOSIM) results of benthic foraminiferal communities based on the three individual stations 180, 24, and 34. "Between" value is used to indicate the dissimilarity among all three of them.

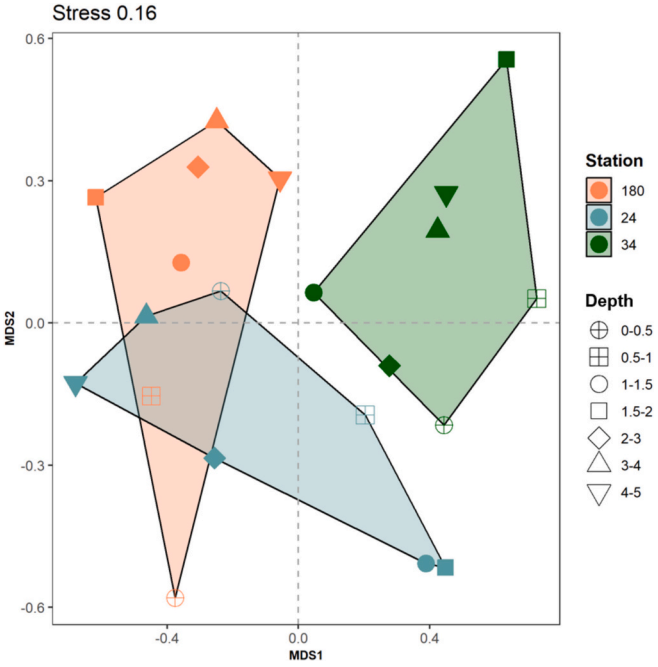

Fig. 11. Non metric-Multidimensional Scaling (NMDS) analysis plot. Stations are represented by different colors and the depth levels within stations by various shapes.

4. Discussions

Through the analysis of living benthic foraminiferal assemblages, this study aims to explore the spatial distribution patterns of communities within Edisto Inlet and to identify the key environmental drivers shaping their structure. Given the point-based nature of the sampling, the results should be interpreted as a temporal snapshot of the inlet at the time of collection.

The integration of environmental and biological data offers a

comprehensive overview of the ecological status of the system, emphasizing the influence of sedimentological characteristics, depositional dynamics, and local hydrography on foraminiferal distribution. Multivariate statistical analyses reveal a clear spatial structuring of the foraminiferal communities. In particular, the ANOSIM results indicate that differences between stations are significantly greater than the variability within each station (Fig. 10). These patterns are supported by the NMDS, which shows a clear separation between stations 34 and 180 and a partial overlap between 24 and 180, indicating some compositional affinity (Fig. 11). This confirms a marked spatial structuring of foraminiferal communities in relation to geochemical and physical parameters, with each station providing distinct ecological niches.

Physico-chemical profiles of the water column reveal a stratification pattern typical of Antarctic fjord systems (Pan et al., 2019; Höfer et al., 2019). The upper ~250 m are characterized by marked variability in temperature and salinity, likely reflecting the influence of glacial meltwater and surface freshwater input. Below this layer, the water column becomes more homogeneous, with stable temperature and salinity values. This vertical transition marks the presence of a well-defined pycnocline, which limits vertical mixing between surface and deep waters. As shown in Fig. 2, the major water masses of the Ross Sea (AASW and mCDW) do not appear to directly influence the circulation within the inlet.

Dissolved oxygen concentrations are highest in the surface layer (~0–50 m), due to atmospheric exchange and photosynthetic activity, and gradually decrease with depth, consistent with reduced ventilation and the remineralization of sinking organic matter. These observations, in line with previous studies (Tesi et al., 2020; Di Roberto et al., 2023; Finocchiaro et al., 2005; Battaglia et al., 2024) and supported by SAR imagery, suggest that Edisto Inlet functions as a semi-enclosed fjord system with significant organic matter accumulation on the seafloor, potentially leading to oxygen-depleted conditions below 250 m waterdepth.

Based on the integration of biological and environmental parameters, three distinct zones can be identified along the Edisto Inlet: (1) an outer fjord zone (station 180), (2) a transitional zone (station 24), and (3) an inner fjord zone (station 34) (Fig. 6). In the following sections, each of these zones will be described and discussed in detail, focusing on the specific environmental settings and the response of living benthic foraminiferal communities to these conditions.

4.1. Outer zone of the inlet (station 180)

Station 180 is located at the fjord entrance, where oceanographic and physico-chemical data indicate a well-oxygenated environment with a high-energy regime and limited organic matter preservation compared to the inner fjord (Figs. 4, 5). This energetic hydrodynamic regime promotes the lowest sedimentation rate among the three sites, and sediment reworking, as indicated by the presence of bioturbation in the surface layers (the upper 4 cm of the core) (Fig. 5).

These conditions reflect active benthic communities and efficient ventilation, which together hinder the accumulation and preservation of labile organic matter (Meyers, 1997; Lamb et al., 2006). In fact, organic carbon content at station 180 is low, and the C/N ratio is relatively high (Fig. 6), indicating the presence of reworked, degraded organic matter with low reactivity. The dominance of terrigenous and glaciogenic inputs, supported by the high value of magnetic susceptibility (Fig. 5), further justified the interpretation of this site as an outer-fjord depositional setting strongly influenced by tidal currents and meltwater-driven sediment transport (Battaglia et al., 2024).

These environmental conditions influence the benthic foraminiferal community, which displays high species richness (51 taxa), overall abundance (637 individuals/cm^3), and a high Simpson diversity index ($D' = 0.9541$), indicative of a well-structured and ecologically diverse assemblage, typically associated with relatively stable environmental conditions (Table 2). However, the Dominance value (0.4587) and the moderate Evenness (0.5969) suggest a moderately heterogeneous habitat, where localized environmental pressures (low pH, hydrodynamic conditions) or resource availability (i.e., low quality OM) may favor the proliferation of few opportunistic taxa, while allowing the persistence of a diverse but less abundant community. This pattern points to a system that, while generally stable, may be subject to occasional or localized disturbances.

In particular, among the agglutinated taxa, *M. arenacea* (Plate II) was particularly abundant. Although taxonomically related to miliolids, this taxon possesses an agglutinated rather than imperforate calcareous test and is an indicator of enhanced carbonate dissolution (Ishman and Szymcek, 2013; Galli et al., 2023). Supporting evidence for this interpretation includes increasing relative abundance of other agglutinated taxa, such as *Portatrochammina antarctica*, *Pseudobolivina antarctica*, and *N. dentaliniformis* (Plates I and II). These opportunistic species typically inhabit coarse-grained, well-oxygenated, oligotrophic sediments in terrigenous-dominated environments such as the Weddell Sea and Admiralty Bay (Murray and Pudsey, 2004; Rodrigues et al., 2015).

Despite this, pH values recorded at station 180 reach surface levels of 7.63, and calcareous specimens found in this site remain well-preserved, suggesting preservation is not severely compromised.

Thus, the presence of a higher proportion of agglutinated species could be justified by the release of CO_2 during sea-ice formation and limited winter gas exchange make brines corrosive, inhibiting calcareous shell formation (Søren et al., 2011). Moreover, it could be a matter of competition for organic matter, which is scarce; in such conditions, agglutinated foraminifera may be more competitive and resilient (Dessandier et al., 2019; Kuhnt et al., 1996; Nardelli et al., 2023).

Similar foraminiferal patterns, characterized by a dominance of agglutinated over calcareous foraminifera, have also been reported under open-marine settings rich in diatoms and organic matter, particularly in association with corrosive High-Salinity Shelf Water (HSSW) (Capotondi et al., 2018; Majewski et al., 2020; Melis and Salvi, 2009), or under cooler conditions indicative of more modified CDW (Lehrmann et al., 2025).

Within the calcareous assemblages, *T. angulosa* (Plate I) dominated the assemblages. This epifaunal taxon is characteristic of shallow subantarctic environments with coarse substrates along the continental shelf (Hayward et al., 2007). Its presence is consistent with the high-energy conditions at this site, as it is known to tolerate strong bottom currents and turbulent hydrodynamic regimes (Murray, 2006; Ishman and Szymcek, 2013; Melis and Salvi, 2020).

Another key component of the assemblage at station 180 is the monothalamous foraminifera, particularly species such as *Micrometula* sp., *P. magnetica,* and *H. hirudinea*. These organic-walled morphotypes are common across various parts of the Ross Sea (Gooday et al., 1996; Violanti, 1996; Majewski et al., 2015; Holzmann et al., 2022, 2025; Pawlowski and Majewski, 2011). For instance, *H. hirudinea* has been reported in the Ezcurra Inlet (King George Island), where it was associated with high concentrations of suspended particulate matter and coarse sediments (Rodrigues et al., 2010). Similarly, *Micrometula* has been identified as an indicator of glacier-proximal conditions in Hornsund Fjord, Svalbard (Pawłowska et al., 2016). Their widespread occurrence in polar settings (Gooday et al., 2004;Sabbatini et al., 2007; Caridi et al., 2021) suggests strong adaptation to high-latitude environments and tolerance to stressors such as sea-ice cover, freshwater influx, and stratified water columns. Comparable environmental conditions are found at station 180, where enhanced hydrodynamic energy leads to increased turbidity and the accumulation of coarse, glaciogenic sediment derived from the nearby glacier front (Battaglia et al., 2024).

4.2. Middle section of the inlet (station 24)

The combination of a relatively high sediment accumulation rate and fine-grained, poorly consolidated sediments indicates enhanced particle flux and sustained sedimentation at this site. High sediment porosity and

water content further suggest recent and unconsolidated deposition (Fig. 5). Surface sediment heterogeneity, characterized by alternating patches of olive and very dark grey mud, is likely associated with diatom-rich layers and reflects episodic pulses of marine organic matter reaching the seafloor (Battaglia et al., 2024; Tesi et al., 2020).

The accumulation of organic material at this site promotes intense microbial degradation and early diagenetic processes, leading to rapid oxygen consumption within the sediments and the development of suboxic conditions below the sediment–water interface. This interpretation is supported by redox profiles showing a rapid transition from oxic to suboxic conditions within the upper sediment layers, as well as by slight pH decreases with depth (Fig. 5), consistent with organic matter remineralization under suboxic conditions (Arndt et al., 2013; Hoogakker et al., 2025).

Geochemical data further corroborate this interpretation (Fig. 6). Moderate organic carbon contents that decrease with depth, together with C/N ratios indicative of predominantly fresh marine-derived, relatively labile organic matter, point to active degradation processes. Isotopic and elemental signatures suggest a mainly marine organic matter source, likely of diatom origin, with minor old terrestrial inputs and additional modification by early diagenetic alteration (Tesi et al., 2020).

Overall, station 24 reflects the intermediate position of this site within the fjord system: a depositional environment where organic matter supply is significant, but where suboxic conditions and early diagenetic processes already play a key role in shaping sediment geochemistry and benthic habitat characteristics.

The benthic foraminiferal assemblage mirrors this transitional setting, showing reduced abundance (193 ind. cm^{-3}) and diversity (29 species) relative to the outer fjord (Table 2). Two key patterns emerge (Figs. 8 and 9): (i) foraminiferal density increases progressively with depth in the sediment, and (ii) calcareous species occur in the lowest percentages, while agglutinated taxa dominate the surface layers and organic-walled foraminifera become predominant at depth.

This vertical distribution is indicative of the prevailing suboxic, chemically stressed conditions. Near the sediment surface, active organic matter degradation likely promotes test dissolution and limits the colonization of calcareous species, while deeper layers, more stable and enriched in degraded diatomaceous material, provide a suitable microhabitat for opportunistic forms. Alternatively, this observed "reverse" pattern may reflect the early stages of recolonization following a rapid depositional event driven by the sinking of organic and lithic particles originally trapped at the base of sea ice during its seasonal melt, which led to the burial of pre-existing surface assemblages. In this context, Nardelli et al. (2023) experimentally demonstrated that foraminifera can rapidly migrate following sedimentary burial to re-establish their preferred living position beneath the newly formed sediment–water interface; however, in the case of abrupt and thick burial events, a longer timescale is required to reach a resilient state. Further support for this interpretation comes from Galli et al. (2025), who analysed samples collected at the same sites but processed using a different staining method (Rose Bengal); their results likewise show the same vertical distribution of living foraminifera.

The surface foraminiferal assemblage at station 24 is dominated by agglutinated species such as *P. batrami* and *Portatrochammina antarctica*, taxa typically associated with low-energy environments and weak bottom currents (Majewski and Anderson, 2009; Capotondi et al., 2020; Galli et al., 2023; Galli et al., 2025). This faunal pattern is consistent with the local oceanographic conditions, as measurements indicate bottom current velocities significantly lower than at station 180 (Fig. 4), which likely favors the settlement and persistence of these agglutinated taxa in the surface sediments. A marked shift in community composition is observed with increasing sediment depth, with monothalamous foraminifera, particularly *Psammosphaerid* spp., *Psammosphaera magnetica*, *Hippocrepinella hirudinea*, and *Tinogullmia* spp. (Plate III), becoming progressively dominant (Fig. 8). Although the occurrence of monothalamous taxa at infaunal depths may appear unusual, it is not unprecedented. In this respect, the recent study by Demianiuk et al. (2025) is particularly relevant, as it documents monothalamous foraminiferal DNA below 5 cm sediment depth, pointing to a deeper infaunal extension than previously recognized.

Soft-shelled monothalamous foraminifera are widespread in Arctic and Antarctic sediments, where benthic assemblages commonly reflect environmental stress, physical disturbance, and opportunistic colonization. At high latitudes, their distribution is closely linked to variable organic matter input, low temperatures, and unstable habitats such as fjords and polar shelves (Gooday, 2002; Korsun, 2002). Many of these taxa exhibit opportunistic life strategies that enable rapid colonization under fluctuating organic supply and hypoxic conditions (Gooday and Jorissen, 2012). *Psammophaga* species, characterized by a sand-ingesting feeding mode, are typically associated with high phytodetritus availability and seasonal pulses of organic input characteristic of polar systems (Gooday et al., 2005; Pawlowski and Majewski, 2011; Caridi et al., 2021). *Tinogullmia* species commonly occur in fjord and marginal sea environments marked by sediment instability and variable oxygenation, whereas *Hippocrepinella hirudinea*, reported from both Arctic (Svalbard) and Antarctic (McMurdo Sound) settings, exhibits distinct regional populations but a consistent association with environmentally stressed polar habitats (Pawlowski et al., 2008).

Taken together, these taxa function as opportunistic indicators of environmental stress at high latitudes, reflecting adaptations to variable organic matter supply, hypoxia, and sediment instability, and thus represent reliable markers of disturbance in polar benthic systems.

4.3. Inner section of the inlet (station 34)

Station 34, located in the innermost part of the Edisto Inlet, is characterized by strongly anoxic conditions and recent, fine-grained, highly hydrated sedimentation. Situated near the Edisto Glacier, at the edge of the deepest and most sheltered part of the inlet (~600 m depth; Fig. 1; Table 1), this site corresponds to a major sediment accumulation area. Extremely high sediment porosity and water content indicate very recent and poorly consolidated deposition, while the absence of bioturbation suggests minimal bottom-water ventilation and limited physical disturbance (Fig. 5). The strongly reduced conditions observed at this site, with negative redox potentials already at the sediment surface, indicate an extremely low-oxygen environment that constrains aerobic organic matter degradation. Under these conditions, organic matter is more efficiently buried and preserved within the sediments. The progressive darkening of sediments with depth and the strong hydrogen sulfide odor, point to intense anaerobic microbial activity. Geochemical indicators further support this interpretation (Figs. 5, 6). High organic carbon contents that decrease only slightly with depth, together with relatively stable C/N ratios, indicate sustained accumulation of predominantly marine-derived organic matter. Markedly depleted $\delta^{13}C$ values suggest extensive microbial reworking, consistent with the dominance of anaerobic metabolic pathways such as sulfate reduction and, potentially, methanogenesis. Collectively, these characteristics identify Station 34 as the end-member depositional environment within the Edisto Inlet, representing a strongly reducing, low-energy basin where early diagenetic processes exert a primary control on sedimentary biogeochemistry.

From an ecological perspective, such extreme conditions severely limit benthic foraminiferal colonization, allowing only highly tolerant or opportunistic taxa to persist. Despite the extreme environmental conditions, a small community of living foraminifera was found at this station, characterized by a low taxonomic diversity value (115 individuals/cm^3 per 23 different species; Table 2). Both the Dominance and Simpson indices indicate a less abundant but well-balanced community, which is characteristic of an extreme environment.

However, the uppermost sediment layers contain calcareous species such as *G. biora* and G. *subglobosa*. *Globocassidulina subglobosa* (Plate I)

has been described as an opportunistic infaunal taxon responding positively to high organic carbon fluxes (Kyrmanidou et al., 2018), whereas *G. biora* is typically associated with high sedimentation rates and sub–ice-shelf environments (Melis and Salvi, 2020). Members of the genus *Globocassidulina* have also been linked to oxygen-poor conditions (Bernhard, 1993). In addition, *B. pseudopunctata* is known to be an opportunistic infaunal species related to environments rich in organic matter content and phytodetritus and that can thrive even in anoxic conditions (Majewski, 2013).

Interestingly, although calcareous forms remain a minority, their relative abundance at station 34 exceeds that at the outer sites (Fig. 9). This may be related to the notably higher pH recorded at this station (8.47), compared to 7.52 and 7.77 at stations 24 and 180, respectively. Nonetheless, several calcareous specimens (*B. pseudopunctata, G. biora, G. subglobosa, Pyrgo* sp.) exhibited partially or almost completely dissolved tests, likely due to localized acidification driven by sulfide accumulation and other by-products of anaerobic metabolism. This dissolution hampered species identification, occasionally limiting classification to the genus level. The proportion of organic-walled forms was also low, possibly reflecting their tendency to suspend metabolic activity under extreme stress (Gooday et al., 1996; Holzmann et al., 2021). Among the species found at station 34, agglutinated taxa such as *P. bartrami* and *Pseudobolivina antarctica* were also identified. These epifaunal species are typically associated with environments characterized by high carbonate dissolution, elevated organic matter accumulation on the seafloor, and, due to their fragile test structure, low-energy, sluggish circulation regimes (Anderson, 1975; Violanti, 2000; Majewski and Anderson, 2009; Majewski, 2010; Majewski et al., 2020). This interpretation is strongly supported by oceanographic measurements: Lowered Acoustic Doppler Current Profilers (LADCP) recorded the lowest water mass velocities at this site, with a maximum speed of only 0.05 m/s (Fig. 4), confirming that the combination of extremely low-energy conditions and the accumulation of buried organic matter favors the persistence of these fragile agglutinated foraminifera.

All these evidences highlight that benthic foraminifera can survive in this extreme environment. In fact, previous studies have reported that foraminifera possess specific physiological and behavioral adaptations that allow them not only to tolerate, but in some cases to thrive under such stressors. As noted by Glock (2023), certain foraminiferal species can survive in anoxic environments through specialized strategies, including heterotrophic denitrification observed in *Globobulimina* species, the retention of functional kleptoplasts acquired from ingested diatoms, and the ability to enter dormant states during prolonged periods of oxygen depletion. In addition, recent studies using molecular and transcriptomic approaches (e.g., Orsi et al., 2020; Gomaa et al., 2021) have further expanded our understanding of foraminiferal adaptations to anoxic environments, revealing the expression of genes related to anaerobic energy pathway (e.g., fermentation, fumarate reduction, [FeFe]-hydrogenase activity, and creatine phosphate-based ATP regeneration), as well as evidence for sustained calcification and phagocytosis under sulfidic and oxygen-depleted conditions.

5. Conclusions

This study provides new insights into the environmental and ecological functioning of Edisto Inlet (Ross Sea, Antarctica), emphasizing how geomorphology, hydrodynamics, sedimentation rates, and biogeochemical factors collectively shape benthic foraminiferal assemblages. By integrating foraminiferal, sedimentological, and oceanographic data, three distinct environmental sectors were identified within the inlet: outer (station 180), middle (station 24), and inner (station 34), each with characteristic habitat conditions and benthic communities. The outer section is characterized by stronger bottom currents and high-energy hydrodynamic conditions, which enhance sediment winnowing and maintain well-oxygenated surface sediments. These conditions favor agglutinated species, including *Miliammina arenacea*, an indicator of carbonate dissolution processes, along with other taxa such as *Portatrochammina antarctica* and *Pseudobolivina antarctica*. Nevertheless, pH values are around 7.63, and well-preserved calcareous species, such as *Trifarina angulosa*, are present, as well as organic-walled forms like *Micrometula* sp. This suggests that the abundance of agglutinated taxa is mainly driven by ecological factors, such as the limited availability of organic matter, which may offer a competitive advantage to agglutinated foraminifera, often more resilient and opportunistic in oligotrophic environments. Station 24 represents a transitional, mid-fjord environment with moderate sedimentation rates (SAR = 0.169 cm yr^{-1}) and weaker bottom currents (~0.14 m/s). Surface sediments are highly porous and enriched in organic matter, promoting suboxic conditions in the upper layers. Foraminiferal abundance and diversity are lower than in the outer fjord, with agglutinated taxa such as *Paratrochammina bartrami* and *Portatrochammina antarctica* dominating the surface sediments. In deeper layers, monothalamous species including *Tinogullmia* sp. and *Psammophaga magnetica* increase in abundance, reflecting opportunistic colonization in organic-rich sediments where redox conditions are less stressful. Moderate pH values, partial oxygen depletion, and early diagenetic alteration create a heterogeneous habitat that shapes community composition. The innermost section experiences extremely low-energy conditions, very weak currents (~0.05 m/s), and the highest sedimentation rates, as it is located at the edge of a natural depositional depression. Surface sediments are highly hydrated (Φ = 0.96), with intense microbial activity leading to strongly reduced redox potential (Eh ≈ −449 mV) and suboxic to anoxic conditions. Organic matter is efficiently buried and preserved, with $\delta^{13}C$ values and stable C/N ratios reflecting marine-derived, partially degraded OM. Opportunistic calcareous species such as *Globocassidulina biora* and *G. subglobosa* persist in these oxygen-depleted, organic-rich sediments. Station 34 thus represents an end-member of the fjord's ecological and geochemical gradient, acting as a hotspot of early diagenetic processes, including sulfate reduction and potentially methanogenesis.

Overall, the observed spatial variability along Edisto Inlet clearly demonstrates that benthic foraminiferal communities are tightly linked to local environmental gradients. Differences in hydrodynamic energy, sedimentation rates, organic matter input, pH, and redox conditions drive the composition, diversity, and vertical distribution of taxa. These results provide a baseline for understanding ecological functioning in Antarctic fjord-like systems and can inform future studies on how polar coastal ecosystems respond to environmental change.

Declaration of generative AI and AI-assisted technologies in the manuscript preparation process

During the preparation of this work the author(s) used ChatGPT in order to improve language and reduce verbosity. After using this tool/service, the author(s) reviewed and edited the content as needed and take(s) full responsibility for the content of the published article.

CRediT authorship contribution statement

F. Caridi: Writing – review & editing, Writing – original draft, Visualization, Project administration, Methodology, Conceptualization. **L. Langone:** Writing – review & editing, Funding acquisition, Project administration. **A. Sartini:** Investigation, Formal analysis, Visualization. **C. Morigi:** Conceptualization, Supervision, Writing – review & editing. **G. Galli:** Formal analysis, Visualization, Writing – review & editing. **P. Giordano:** Writing – review & editing, Investigation. **M. Bensi:** Writing – review & editing, Investigation. **V. Kovacevic:** Writing – review & editing, Investigation. **L. Ursella:** Investigation, Writing – review & editing. **N. Krauzig:** Investigation. **A. Sabbatini:** Writing – review & editing, Supervision, Methodology, Conceptualization.

Declaration of competing interest

The authors declare that they have no known competing financial interests or personal relationships that could have appeared to influence the work reported in this paper.

Acknowledgements

We express our sincere gratitude to the R/V Laura Bassi crew and OGS technicians for their support in sampling activities during the PNRA XXXVIII Antarctic Expedition, Leg 2. Special thanks are extended to Dr. Riccardo Scipinotti for the invaluable logistic assistance. This paper represents a contribution from the PNRA19_00069 LASAGNE project. The present work was part of Alessandro Sartini's Master's thesis.

Appendix A. Supplementary data

Supplementary data to this article can be found online at https://doi.org/10.1016/j.marmicro.2026.102553.

Data availability

Data will be made available on request.

References

Ainley, D.G., Morandini, V., Salas, L., Nur, N., Rotella, J., Barton, K., Lyver, P.O., Goetz, K.T., Larue, M., Foster-Dyer, R., Parkinson, C.L., Arrigo, K.R., Van Dijken, G., Beltran, R.S., Kim, S., Brooks, C., Kooyman, G., Ponganis, P.J., Shanhun, F., Anderson, D.P., 2024. Response of indicator species to changes in food web and ocean dynamics of the Ross Sea, Antarctica. Antarct. Sci. 36 (5), 290–318. https://doi.org/10.1017/S0954102024000191.

Altenbach, A.V., 1992. Short term processes and patterns in the foraminiferal response to organic flux rates. Mar. Micropaleontol. 19 (2), 119–129. https://doi.org/10.1016/0377-8398(92)90024-E.

Alve, E., Bernhard, J.M., 1995. Vertical migratory response of benthic foraminifera to controlled oxygen concentrations in an experimental mesocosm. Mar. Ecol. Prog. Ser. 116, 137–151. https://doi.org/10.3354/meps116137.

Anderson, J.B., 1975. Ecology and distribution of foraminifera in the Weddell Sea of Antarctica. Micropaleontology 21 (1), 69–96.

Arndt, S., Jørgensen, B.B., LaRowe, D.E., Middelburg, J.J., Pancost, R.D., Ragnier, P., 2013. Quantifying the degradation of organic matter in marine sediments: a review and synthesis. Earth Sci. Rev. 123, 53–86. https://doi.org/10.1016/j.earscirev.2013.02.008.

Battaglia, F., De Santis, L., Baradello, L., Colizza, E., Rebesco, M., Kovacevic, V., Ursella, L., Bensi, M., Accettella, D., Morelli, D., Corradi, N., Falco, P., Krauzig, N., Colleoni, F., Gordini, E., Caburlotto, A., Langone, L., Finocchiaro, F., 2024. The discovery of the southernmost ultra-high-resolution Holocene paleoclimate sedimentary record in Antarctica. Mar. Geol. 467, 107189. https://doi.org/10.1016/j.margeo.2023.107189.

Bernhard, J.M., 1993. Experimental and field evidence of Antarctic foraminiferal tolerance to anoxia and hydrogen sulfide. Mar. Micropaleontol. 20 (3–4), 203–213. https://doi.org/10.1016/0377-8398(93)90033-T.

Bernhard, J.M., Habura, A., Bowser, S.S., 2006. An endobiont-bearing allogromiid from the Santa Barbara Basin: Implications for the early diversification of foraminifera. Journal of Geophysical Research. Biogeosciences 111 (G3). https://doi.org/10.1029/2005JG000158.

Bromwich, D.H., Nicolas, J.P., Monaghan, A.J., Lazzara, M.A., Keller, L.M., Weidner, G.A., Wilson, A.B., 2014. Central West Antarctica among the most rapidly warming regions on Earth. Nat. Geosci. 6, 139–145. https://doi.org/10.1038/ngeo1671.

Bromwich, D., Wang, S.H., Zou, X., Ensign, A., 2025. An updated reconstruction of Antarctic near-surface air temperatures at monthly intervals since 1958. Earth Syst. Sci. Data 17 (6), 2953–2962. https://doi.org/10.5194/essd-17-2953-2025.

Capotondi, L., Bergami, C., Giglio, F., Langone, L., Ravaioli, M., 2018. Benthic foraminifera distribution in the Ross Sea (Antarctica) and its relationship to oceanography. Boll. Soc. Paleontol. Ital. 57 (3), 187–202. https://doi.org/10.4435/BSPI.2018.12.

Capotondi, L., Bonomo, S., Budillon, G., Giordano, P., Langone, L., 2020. Living and dead benthic foraminiferal distribution in two areas of the Ross Sea (Antarctica). Rendiconti Lincei. Scienze Fisiche e Naturali 31 (4), 1037–1053. https://doi.org/10.1007/s12210-020-00949-z.

Caridi, F., Sabbatini, A., Bensi, M., Kovačević, V., Lucchi, R.G., Morigi, C., Povea, P., Negri, A., 2021. Benthic foraminiferal assemblages and environmental drivers along the Kveithola Trough (NW Barents Sea). J. Mar. Syst. 224, 103616. https://doi.org/10.1016/j.jmarsys.2021.103616.

Caridi, F., Sabbatini, A., Morigi, C., 2023. Monothalamous soft-shelled foraminiferal image dataset from the Kveithola Trough (NW Barents Sea). Data Brief 50, 109603. https://doi.org/10.1016/j.dib.2023.109603.

Castagno, P., Falco, P., Dinniman, M.S., Spezie, G., Budillon, G., 2017. Temporal variability of the circumpolar deep water inflow onto the Ross Sea continental shelf. J. Mar. Syst. 166 (37–49), 2017. https://doi.org/10.1016/j.jmarsys.2016.05.006.

Clarke, K.R., Ainsworth, M., 1993. A method of linking multivariate community structure to environmental variables. Mar. Ecol. Prog. Ser. 205–219.

Clem, K.R., et al., 2020. Record warming at the South Pole during the past three decades. Nat. Clim. Chang. 10 (8), 762–770. https://doi.org/10.1038/s41558-020-0815-z.

Covelli, S., Langone, L., Acquavita, A., Piani, R., Emili, A., 2012. Historical flux of mercury associated with mining and industrial sources in the Marano and Grado Lagoon (northern Adriatic Sea). Estuar. Coast. Shelf Sci. 113, 7–19. https://doi.org/10.1016/j.ecss.2011.12.038.

Demianiuk, E., Baca, M., Popović, D., Barrenechea Angeles, I., Nguyen, N.L., Pawlowski, J., Anderson, J.B., Majewski, W., 2025. Sedimentary ancient DNA insights into foraminiferal diversity near the grounding line in the western Ross Sea, Antarctica. Biogeosciences 22 (11), 2601–2620. https://doi.org/10.5194/bg-22-2601-2025.

Dessandier, P.A., Borrelli, C., Kalenitchenko, D., Panieri, G., 2019. Benthic foraminifera in arctic methane hydrate bearing sediments. Front. Mar. Sci. 6, 765. https://doi.org/10.3389/fmars.2019.00765.

Di Roberto, A., Re, G., Scateni, B., Petrelli, M., Tesi, T., Capotondi, L., Morigi, C., Galli, G., Colizza, E., Melis, R., Torricella, F., Giordano, P., Giglio, F., Gallerani, A., Gariboldi, K., 2023. Cryptotephras in the marine sediment record of the Edisto Inlet, Ross Sea: Implications for the volcanology and tephrochronology of northern Victoria Land, Antarctica. Quat. Sci. Adv. 10, 100079. https://doi.org/10.1016/j.qsa.2023.100079.

Ernst, S., van der Zwaan, B., 2004. Effects of experimentally induced raised levels of organic flux and oxygen deple- tion on a continental slope benthic foraminiferal community. Deep Sea Res. Part Oceanogr. Res. Pap. 51, 1709–1739. https://doi.org/10.1016/j.dsr.2004.06.003.

Ernst, S., Duijnstee, I., van der Zwaan, B., 2002. The dynamics of the benthic foraminiferal microhabitat: recovery after experimental disturbance. Mar. Micropaleontol. 46, 343–361. https://doi.org/10.1016/S0377-8398(02)00080-4.

Ernst, S., Bours, R., Duijnstee, I., van der Zwaan, B., 2005. Experimental effects of an organic matter pulse and oxygen depletion on a benthic foraminiferal shelf community. J. Foraminifer. Res. 35, 177–197. https://doi.org/10.2113/35.3.177.

Ernst, S.R., Morvan, J., Geslin, E., Le Bihan, A., Jorissen, F.J., 2006. Benthic foraminiferal response to experimentally induced Erika oil pollution. Mar. Micropaleontol. 61, 76–93. https://doi.org/10.1016/j.marmicro.2006.05.005.

Falco, P., Aulicino, G., Castagno, P., Capozzi, V., de Ruggiero, P., Garzia, A., Ian Ferola, A., Cotroneo, Y., Colella, A., Fusco, G., Pierini, G., Budillon, G., Zambianchi, E., Spezie, G., 2024. Ocean-atmosphere-ice processes in the Ross Sea: a review. Prog. Oceanogr. 202, 102795. https://doi.org/10.1016/j.dsr2.2024.105429.

Finocchiaro, F., Langone, L., Colizza, E., Fontolan, G., Giglio, F. and Tuzzi, E., 2005. Record of the early Holocene warming in a laminated sediment core from Cape Hallett Bay (Northern Victoria Land, Antarctica). Glob. Planet. Chang., 45(1–3), 193–206. doi:https://doi.org/10.1016/j.gloplacha.2004.09.003.

Fossile, E., 2022. Ice-Related Environmental Changes in Arctic Fjords: New Insights from Benthic Foraminifera (Doctoral dissertation,. Université d'Angers.

Frignani, M., Langone, L., Ravaioli, M., Sorgente, D., Alvisi, F., Albertazzi, S., 2005. Fine-sediment mass balance in the western Adriatic continental shelf over a century time scale. Mar. Geol. 222 (1–4), 1–17.

Galli, G., Morigi, C., Melis, R., Di Roberto, A., Tesi, T., Torricella, F., Langone, L., Giordano, P., Colizza, E., Capotondi, L., Gallerani, A., Gariboldi, K., 2023. Paleoenvironmental changes related to the variations of the sea-ice cover during the late Holocene in an Antarctic fjord (Edisto Inlet, Ross Sea) inferred by foraminiferal association. J. Micropalaeontol. 42 (2), 95–115. https://doi.org/10.5194/jm-42-95-2023.

Galli, G., Caridi, F., Giordano, P., Morigi, C., Sabbatini, A., Langone, L., 2025. Community structures and Taphonomic controls on benthic foraminiferal community from an Antarctic Fjord (Edisto Inlet, Victoria Land). EGUsphere 2025, 1–31. https://doi.org/10.5194/egusphere-2025-5204.

Gaździcki, A., Majewski, W., 2003. Recent foraminifera from Goulden Cove of King George Island, Antarctica. Pol. Polar Res. 24 (3), 227–239.

Glock, N., 2023. Benthic foraminifera and gromiids from oxygen-depleted environments–survival strategies, biogeochemistry and trophic interactions. Biogeosciences 20 (16), 3423–3447. https://doi.org/10.5194/bg-20-3423-2023.

Gomaa, F., Utter, D.R., Powers, C., Beaudoin, D.J., Edgcomb, V.P., Filipsson, H.L., Hansel, C.M., Wankel, S.D., Zhang, Y., Bernhard, J.M., 2021. Multiple integrated metabolic strategies allow foraminiferan protists to thrive in anoxic marine sediments. Sci. Adv. 7, eabf1586. https://doi.org/10.1126/sciadv.abf1586.

Gooday, A.J., 2002. Organic-walled allogromiids: aspects of their occurrence, diversity and ecology in marine habitats. J. Foraminifer. Res. 32 (4), 384–399. https://doi.org/10.2113/0320384.

Gooday, A.J., 2003. Benthic foraminifera (Protista) as tools in deep-water palaeoceanography: Environmental influences on faunal characteristics. Adv. Mar. Biol. 46, 1–90. https://doi.org/10.1016/S0065-2881(03)46002-1.

Gooday, A.J., Bowser, S.S., Cedhagen, T., Cornelius, N., Hald, M., Korsun, S., Pawlowski, J., 2005. Monothalamous foraminiferans and gromiids (Protista) from western Svalbard: a preliminary survey. Mar. Biol. Res. 1 (4), 290–312. https://doi.org/10.1080/17451000510019150.

Gooday, A.J., Jorissen, F.J., 2012. Benthic foraminiferal biogeography: Controls on global distribution patterns in deep-water settings. Annu. Rev. Mar. Sci. 4, 237–262. https://doi.org/10.1146/annurev-marine-120709-142737.

Gooday, A.J., Rathburn, A.E., 1999. Temporal variability in living deep-sea benthic foraminifera: a review. Earth Sci. Rev. 46 (1–4), 187–212. https://doi.org/10.1016/S0012-8252(99)00010-0.

Gooday, A.J., Bowser, S.S., Bernhard, J.M., 1996. Benthic foraminiferal assemblages in Explorers Cove, Antarctica: a shallow-water site with deep-sea characteristics. Prog. Oceanogr. 37 (2), 117–166. https://doi.org/10.1016/S0079-6611(96)00007-9.
Gooday, A.J., Bowser, S.S., Cedhagen, T., 2004. Monothalamous foraminiferans and gromiids from western Svalbard: Ecological and taxonomic notes. J. Foramin. Res. 34 (1), 34–48. https://doi.org/10.1080/17451000510019150.
Hammer, Ø., Harper, D.A.T., Ryan, P.D., 2001. PAST: Past: paleontological statistics software package for education and data analysis. Palaeontol. Electron. 4 (1), 9.
Hauck, J., Völker, C., Wang, T., Hoppema, M., 2015. Seasonally different carbon flux changes in the Southern Ocean in response to the Southern Annular Mode. Glob. Biogeochem. Cycles 29 (8), 1238–1253. https://doi.org/10.1002/2015GB005140.
Hayward, B.W., Grenfell, H.R., Sabaa, A.T., Daymond-King, R., 2007. Biogeography and ecological distribution of shallow-water benthic foraminifera from the Auckland and Campbell Islands, subantarctic Southwest Pacific. J. Micropalaeontol. 26 (2), 127–143. https://doi.org/10.1144/jm.26.2.127.
Höfer, J., Giesecke, R., Hopwood, M.J., Carrera, V., Alarcón, E., González, H.E., 2019. The role of water column stability and wind mixing in the production/export dynamics of two bays in the Western Antarctic Peninsula. Prog. Oceanogr. 174, 105–116. https://doi.org/10.1016/j.pocean.2019.01.005.
Holzmann, M., Gooday, A.J., Siemensma, F., Pawlowski, J., 2021. Freshwater and soil foraminifera–a story of long-forgotten relatives. J. Foraminifer. Res. 51 (4), 318–331. https://doi.org/10.2113/gsjfr.51.4.318.
Holzmann, M., Gooday, A.J., Majewski, W., Pawlowski, J., 2022. Molecular and morphological diversity of monothalamous foraminifera from South Georgia and the Falkland Islands: description of four new species. Eur. J. Protistol. 85, 125909. https://doi.org/10.1016/j.ejop.2022.125909.
Holzmann, M., Gooday, A.J., Pawlowski, J., 2025. *Flaviatella* gen. Nov., a new genus of monothalamous foraminifera with a wide geographical and bathymetrical distribution. Prog. Oceanogr., 103589 https://doi.org/10.1016/j.pocean.2025.103589.
Hoogakker, B.A.A., Davis, C., Wang, Y., Kusch, S., Nilsson-Kerr, K., Hardisty, D.S., Jacobel, A., Reyes Macaya, D., Glock, N., Ni, S., Sepúlveda, J., Ren, A., Auderset, A., Hess, A.V., Meissner, K.J., Cardich, J., Anderson, R., Barras, C., Basak, C., Bradbury, H.J., Brinkmann, I., Castillo, A., Cook, M., Costa, K., Choquel, C., Diz, P., Donnenfield, J., Elling, F.J., Erdem, Z., Filipsson, H.L., Garrido, S., Gottschalk, J., Govindankutty Menon, A., Groeneveld, J., Hallmann, C., Hendy, I., Hennekam, R., Lu, W., Lynch-Stieglitz, J., Matos, L., Martínez-García, A., Molina, G., Muñoz, P., Moretti, S., Morford, J., Nuber, S., Radionovskaya, S., Raven, M.R., Somes, C.J., Studer, A.S., Tachikawa, K., Tapia, R., Tetard, M., Vollmer, T., Wang, X., Wu, S., Zhang, Y., Zheng, X.-Y., Zhou, Y., 2025. Reviews and syntheses: Review of proxies for low-oxygen paleoceanographic reconstructions. Biogeosciences 22, 863–957. https://doi.org/10.5194/bg-22-863-2025.
Igarashi, A., Numanami, H., Tsuchiya, Y., Fukuchi, M., 2001. Bathymetric distribution of fossil foraminifera within marine sediment cores from the eastern part of Lützow-Holm Bay, East Antarctica, and its paleoceanographic implications. Mar. Micropaleontol. 42 (3–4), 125–162. https://doi.org/10.1016/S0377-8398(01)00004-4.
Ishman, S.E., Szymcek, P., 2013. Foraminiferal distributions in the former larsen-a ice shelf and Prince Gustav Channel Region, Eastern Antarctic Peninsula margin: a baseline for Holocene paleoenvironmental change. In: Antarctic Peninsula climate Variability: Historical and Paleoenvironmental Perspectives, Antarct. Res. Ser., pp. 239–260. https://doi.org/10.1029/AR079p0239.
Johnson, G.C., 2008. Quantifying Antarctic bottom water and North Atlantic deep water volumes. J. Geophys. Res. 113 (C5), C05019. https://doi.org/10.1029/2007JC004477.
Kennett, J.P., 1966. Foraminiferal evidence of a shallow calcium carbonate solution boundary, Ross Sea. Antarct. Sci. 153 (3732), 191–193.
Kohut, J., Hunter, E., Huber, B., 2013. Small-scale variability of the cross-shelf flow over the outer shelf of the Ross Sea. J. Geophys. Res. Oceans 118 (4), 1863–1876. https://doi.org/10.1002/jgrc.20090.
Korsun, S., 2002. Allogromiids in foraminiferal assemblages on the western Eurasian Arctic shelf. J. Foraminifer. Res. 32 (4), 400–413. https://doi.org/10.2113/0320400.
Kuhnt, W., Moullade, M., Kaminski, M.A., 1996. Ecological structuring and evolution of deep sea agglutinated foraminifera—a review. Rev. Micropaleontol. 39 (4), 271–281. https://doi.org/10.1016/S0035-1598(96)90119-1.
Kyrmanidou, A., Vadman, K.J., Ishman, S.E., Leventer, A., Brachfeld, S., Domack, E.W., Wellner, J.S., 2018. Late Holocene oceanographic and climatic variability recorded by the Perseverance Drift, northwestern Weddell Sea, based on benthic foraminifera and diatoms. Mar. Micropaleontol. 141, 10–22. https://doi.org/10.1016/j.marmicro.2018.03.001.
Lamb, A.L., Wilson, G.P., Leng, M.J., 2006. A review of coastal palaeoclimate and relative sea-level reconstructions using $\delta^{13}C$ and C/N ratios in organic material. Earth Sci. Rev. 75 (1–4), 29–57. https://doi.org/10.1016/j.earscirev.2005.10.003.
Langone, L., The LASAGNE Team, 2024. Environmental factors influencing deposition and preservation of laminated sediments in Edisto Inlet, western Ross Sea (Antarctica). In: EGU General Assembly 2024, Vienna, Austria, 14–19 Apr 2024, EGU24-11258. https://doi.org/10.5194/egusphere-egu24-11258.
Lehrmann, A.A., Totten, R.L., Wellner, J.S., Hillenbrand, C.D., Radionovskaya, S., Comas, R.M., Larter, R.D., Graham, A.G., Kirkham, J.D., Hogan, K.A., Fitzgerald, V., 2025. Recent benthic foraminifera communities offshore of Thwaites Glacier in the Amundsen Sea, Antarctica: implications for interpretations of fossil assemblages. J. Micropalaeontol. 44 (1), 79–105. https://doi.org/10.5194/jm-44-79-2025.
Lombardi, C., Kuklinski, P., Bordone, A., Spirandelli, E., Raiteri, G., 2021. Assessment of annual physico-chemical variability via high-temporal resolution monitoring in an Antarctic Shallow Coastal Site (Terra Nova Bay, Ross Sea). Minerals 11 (4), 374. https://doi.org/10.3390/min11040374.
Lutze, G.F., Coulbourn, W.T., 1984. Recent benthic foraminifera from the continental margin of Northwest Africa: Community structure and distribution. Mar. Micropaleontol. 8 (5), 419–444. https://doi.org/10.1016/0377-8398(84)90002-1.
Mackensen, A., Grobe, H., Kuhn, G., Fu, D.K., 1990. Benthic foraminiferal assemblages from the eastern Weddell Sea between 68 and 73 S: distribution, ecology and fossilization potential. Mar. Micropaleontol. 16 (3–4), 241–283. https://doi.org/10.1016/0377-8398(90)90006-8.
Majewski, W., 2010. Benthic foraminifera from West Antarctic fiord environments: an overview. Pol. Polar Res. 1, 61–82.
Majewski, W., 2013. Benthic foraminifera from Pine island and Ferrero bays, Amundsen Sea. Pol. Polar Res. 34 (1), 1–26. https://doi.org/10.2478/popore-2013-0012.
Majewski, W., Anderson, J.B., 2009. Holocene foraminiferal assemblages from Firth of Tay, Antarctic Peninsula: paleoclimate implications. Mar. Micropaleontol. 73 (3–4), 135–147. https://doi.org/10.1016/j.marmicro.2009.08.003.
Majewski, W., Lecroq, B., Sinniger, F., Pawłowski, J., 2007. Monothalamous foraminifera from Admiralty Bay, King George Island, West Antarctica. Pol. Polar Res. 187–210.
Majewski, W., Bowser, S.S., Pawlowski, J., 2015. Widespread intra-specific genetic homogeneity of coastal Antarctic benthic foraminifera. Polar Biol. 38 (12), 2047–2058. https://doi.org/10.1007/s00300-015-1765-1.
Majewski, W., Pawlowski, J., Zajaczkoeski, M., 2005. Monothalamous foraminifera from West Spitspergen fjords, Svalbard: a brief overview. Pol. Polar Res. 26, 269–285.
Majewski, W., Prothro, L.O., Simkins, L.M., Demianiuk, E.J., Anderson, J.B., 2020. Foraminiferal patterns in deglacial sediment in the western Ross Sea, Antarctica: Life near grounding lines. Paleoceanogr. Paleoclimatol. 35 (5), e2019PA003716. https://doi.org/10.1029/2019PA003716.
Massom, R.A., Stammerjohn, S.E., 2010. Antarctic Sea ice change and variability – Physical and ecological implications. Polar Sci. 4 (2), 149–186. https://doi.org/10.1016/j.polar.2010.05.001.
Melis, R., Salvi, G., 2009. Late Quaternary foraminiferal assemblages from western Ross Sea (Antarctica) in relation to the main glacial and marine lithofacies. Mar. Micropaleontol. 70 (1–2), 39–53. https://doi.org/10.1016/j.marmicro.2008.10.003.
Melis, R., Salvi, G., 2020. Foraminifer and ostracod occurrence in a cool-water carbonate factory of the Cape Adare (Ross Sea, Antarctica): a key lecture for the climatic and oceanographic variations in the last 30,000 years. Geosciences 10 (10), 413. https://doi.org/10.3390/geosciences10100413.
Meyers, P.A., 1997. Organic geochemical proxies of paleoceanographic change. Chem. Geol. 138 (1–2), 289–302. https://doi.org/10.1016/S0146-6380(97)00049-1.
Milam, R.W., Anderson, J.B., 1981. Distribution and ecology of recent benthonic foraminifera of the Adelie-George V continental shelf and slope, Antarctica. Mar. Micropaleontol. 6 (4), 297–325.
Murray, J.W., 2001. The niche of benthic foraminifera, critical thresholds and adaptation to environmental stress. Mar. Micropaleontol. 41 (1–2), 1–7. https://doi.org/10.1016/S0377-8398(00)00057-8.
Murray, J.W., 2006. Ecology and Applications of Benthic Foraminifera. Cambridge University Press, Cambridge.
Murray, J.W., 2014. Ecology and Palaeoecology of Benthic Foraminifera. Routledge.
Murray, J.W., Pudsey, C.J., 2004. Living (stained) and dead foraminifera from the newly ice-free Larsen Ice Shelf, Weddell Sea, Antarctica: Ecology and taphonomy. Mar. Micropaleontol. 53 (1–2), 67–81. https://doi.org/10.1016/j.marmicro.2004.04.001.
Nardelli, M.P., Fossile, E., Peron, O., Howa, H., Mojtahid, M., 2023. Early taphonomy of benthic foraminifera in Storfjorden 'sea-ice factory': the agglutinated/calcareous ratio as a proxy for brine persistence. Boreas 52 (1), 109–123. https://doi.org/10.1111/bor.12592.
Orsi, A.H., Wiederwohl, C.L., 2009. A recount of Ross Sea waters. Deep-Sea Res. II 56 (7–8), 778–795. https://doi.org/10.1016/j.dsr2.2008.10.033.
Orsi, A.H., Whitworth, T., Nowlin, W.D., 1999. On the circulation and stratification of the Weddell Gyre. Deep-Sea Res. I 46 (4), 501–527. https://doi.org/10.1016/0967-0637(93)90060-G.
Orsi, W.D., Morard, R., Vuillemin, A., Eitel, M., Wörheide, G., Milucka, J., Kucera, M., 2020. Anaerobic metabolism of Foraminifera thriving below the seafloor. ISME J. 14, 2580–2594. https://doi.org/10.1038/s41396-020-0708-1.
Pan, B.J., Vernet, M., Reynolds, R.A., Mitchell, B.G., 2019. The optical and biological properties of glacial meltwater in an Antarctic fjord. PLoS One 14 (2), e0211107. https://doi.org/10.1371/journal.pone.0211107.
Pawłowska, J., Zajączkowski, M., Łącka, M., Lejzerowicz, F., Esling, P., Pawlowski, J., 2016. Palaeoceanographic changes in Hornsund Fjord (Spitsbergen, Svalbard) over the last millennium: new insights from ancient DNA. Clim. Past 12 (7), 1459–1472. https://doi.org/10.5194/cp-12-1459-2016.
Pawlowski, J., Majewski, W., 2011. Magnetite-bearing foraminifera from Admiralty Bay, West Antarctica, with description of *Psammophaga magnetica*, sp. nov. J. Foraminifer. Res. 41 (1), 3–13. https://doi.org/10.2113/gsjfr.41.1.3.
Pawlowski, J., Majewski, W., Longet, D., Guiard, J., Cedhagen, T., Gooday, A.J., Korsun, S., Habura, A.A., Bowser, S.S., 2008. Genetic differentiation between Arctic and Antarctic monothalamous foraminiferans. Polar Biol. 31 (10), 1205–1216. https://doi.org/10.1007/s00300-008-0459-3.
Pucci, F., Geslin, E., Barras, C., Morigi, C., Sabbatini, A., Negri, A., Jorissen, F.J., 2009. Survival of benthic foraminifera under hypoxic conditions: Results of an experimental study using the CellTracker Green method. Mar. Pollut. Bull. 59 (8–12), 336–351. https://doi.org/10.1016/j.marpolbul.2009.08.015.
Rodrigues, A.R., Maluf, J.C.C., de Santis Braga, E., Eichler, B.B., 2010. Recent benthic foraminiferal distribution and related environmental factors in Ezcurra Inlet, King George Island, Antarctica. Antarct. Sci. 22 (4), 343–360. https://doi.org/10.1017/S0954102010000179.

R Core Team. R: A language and environment for statistical computing. R Foundationfor Statistical Computing. https://www.R-project.org/.
Rodrigues, A.R., de Santis Braga, E., Eichler, B.B., 2015. Living foraminifera in the shallow waters of Admiralty Bay: distributions and environmental factors. J. Foraminifer. Res. 45 (2), 128–145. https://doi.org/10.2113/gsjfr.45.2.128.
Rogers, A.D., Frinault, B.A., Barnes, D.K.A., Bindoff, N.L., Downie, R., Ducklow, H.W., Friedlaender, A.S., Hart, T., Hill, S.L., Hofmann, E.E., Linse, K., McMahon, C.R., Murphy, E.J., Pakhomov, E.A., Reygondeau, G., Staniland, I.J., Wolf-Gladrow, D.A., Wright, R.M., 2020. Antarctic futures: an assessment of climate-driven changes in ecosystem structure, function, and service provisioning in the Southern Ocean. Annu. Rev. Mar. Sci. 12 (1), 87–120. https://doi.org/10.1146/annurev-marine-010419-011028.
Sabbatini, A., Morigi, C., Ravaioli, M., Negri, A., 2004. Abyssal benthic foraminifera in the Polar Front region (Pacific sector): Faunal composition, standing stock and size structure. Chem. Ecol. 20 (sup1), S117–S129. https://doi.org/10.1080/02757540410001655387.
Sabbatini, A., Morigi, C., Negri, A., Gooday, A.J., 2007. Distribution and biodiversity of stained monothalamous foraminifera from Tempelfjord, Svalbard. J. Foramin. Res. v37 (2), 93–106. https://doi.org/10.2113/gsjfr.37.2.93.
Sabbatini, A., Bazzaro, M., Caridi, F., De Vittor, C., Esposito, V., Lucchi, R.G., Negri, A., Morigi, C., 2023. Benthic Foraminifera and Productivity Regimes in the Kveithola Trough (Barents Sea) ecological implications in a changing arctic and actuopaleontological meaning. J. Mar. Sci. Eng. 11 (2), 237.
Sabine, C.L., Feely, R.A., Gruber, N., Key, R.M., Lee, K., Bullister, J.L., Wanninkhof, R., Wong, C.S., Wallace, D.W.R., Tilbrook, B., Millero, F.J., Peng, T.-H., Kozyr, A., Ono, T., Rios, A.F., 2004. The oceanic sink for anthropogenic CO_2. Science 305 (5682), 367–371. https://doi.org/10.1126/science.1097403.
Saraswat, R., Nigam, R., Li, T., Griffith, E.M., 2017. Marine paleoclimatic proxies: a shift from qualitative to quantitative estimation of seawater parameters. Palaeogeogr. Palaeoclimatol. Palaeoecol. 483, 1–5. https://doi.org/10.1016/j.palaeo.2017.05.036.
Schlitzer, R., 2025. Ocean Data VIew. https://odv.awi.de.
Silvano, A., Purkey, S., Gordon, A.L., Castagno, P., Stewart, A.L., Rintoul, S.R., Lee, W.S., 2023. Observing Antarctic bottom water in the Southern Ocean. Front. Mar. Sci. 10, 1221701. https://doi.org/10.3389/fmars.2023.1221701.
Smith Jr., W.O., Dinniman, M.S., Hofmann, E.E., Klinck, J.M., 2014. The effects of changing winds and temperatures on the oceanography of the Ross Sea in the 21st century. Geophys. Res. Lett. 41 (4), 1183–1190. https://doi.org/10.1002/2014GL059311.
Somerfield, P.J., Clarke, K.R., Gorley, R.N., 2021. Analysis of similarities (ANOSIM) for 3-way designs. Austr. Ecol. 46 (6), 927–941. https://doi.org/10.1111/aec.13083.
Søren, R., Bendtsen, J., Delille, B., Dieckmann, G.S., Glud, R.N., Kennedy, H., Mortensen, J., Papadimitriou, S., Thomas, D.N., Tison, J.L., 2011. Sea ice contribution to the air–sea CO2 exchange in the Arctic and Southern Oceans. Tellus B 63 (5), 823–830. https://doi.org/10.1111/j.1600-0889.2011.00571.x.
Stammerjohn, S.E., Scambos, T.A., 2020. Warming reaches the south pole. Nat. Clim. Chang. 10 (8), 710–711. https://doi.org/10.1038/s41558-020-0827-8.
Tesi, T., Langone, L., Goni, M.A., Wheatcroft, R.A., Miserocchi, S., Bertotti, L., 2012. Early diagenesis of recently deposited organic matter: A 9-yr time-series study of a flood deposit. Geochim. Cosmochim. Acta 83, 19–36. https://doi.org/10.1016/j.gca.2011.12.026.
Tesi, T., Belt, S.T., Gariboldi, K., Muschitiello, F., Smik, L., Finocchiaro, F., Giglio, F., Colizza, E., Gazzurra, G., Giordano, P., Morigi, C., Capotondi, L., Nogarotto, A., Koseoglu, D., Di Roberto, A., Gallerani, A., Langone, L., 2020. Resolving Sea ice dynamics in the North-Western Ross Sea during the last 2.6 ka: from seasonal to millennial timescales. Quat. Sci. Rev. 237, 106299. https://doi.org/10.1016/j.quascirev.2020.106299.
The MathWorks Inc., 2024. MATLAB version: 9.13.0 (R2020b). https://www.mathworks.com (last access: 1 January 2024).
Turner, J., Colwell, S.R., Marshall, G.J., Lachlan-Cope, T.A., Carleton, A.M., Jones, P.D., Lagun, V., Reid, P.A., Iagovkina, S., 2005. Antarctic climate change during the last 50 years. Int. J. Climatol. 25 (3), 279–294. https://doi.org/10.1002/joc.1130.
Turner, J., Lu, H., King, J., Marshall, G.J., Phillips, T., Bannister, D., Colwell, S., 2021. Extreme temperatures in the Antarctic. J. Clim. 34 (7), 2653–2668. https://doi.org/10.1175/JCLI-D-20-0538.1.
Van der Zwaan, G.J., Duijnstee, I.A.P., den Dulk, M., Ernst, S.R., Jannink, N.T., Kouwenhoven, T.J., 1999. Benthic foraminifers: Proxies or problems? A review of paleocological concepts. Earth Sci. Rev. 46 (1–4), 213–236. https://doi.org/10.1016/S0012-8252(99)00011-2.
Vaughan, D.G., Marshall, G.J., Connolley, W.M., Parkinson, C., Mulvaney, R., Hodgson, D.A., Turner, J., 2003. Recent rapid regional climate warming on the Antarctic Peninsula. Clim. Chang. 60 (3), 243–274. https://doi.org/10.1023/A:1026021217991.
Violanti, D., 1996. Taxonomy and distribution of recent benthic foraminifers from Terra Nova Bay (Ross Sea, Antarctica), oceanographic campaign 1987/1988. Palaeontogr. Ital. 83, 25–71.
Violanti, D., 2000. Morphogroup analysis of recent agglutinated foraminifers off Terra Nova Bay, Antarctica (Expedition 1987–1988). In Ross Sea Ecology: Italiantartide Expeditions (1987–1995) (pp. 479–492). Berlin, Heidelberg: Springer Berlin Heidelberg. doi:https://doi.org/10.1007/978-3-642-59607-0_34.
Xie, C., Zhang, Z., Chen, Y., Wang, C., 2025. Substantial contraction of Dense Shelf Water in the Ross Sea under future climate scenarios. Geophys. Res. Lett. 52 (1), e2024GL112581. https://doi.org/10.1029/2024GL112581.
Xu, Q.B., Yang, L.J., Gao, Y.S., Sun, L.G., Xie, Z.Q., 2021. 6000-year reconstruction of Modified Circumpolar Deep Water intrusion in the Ross Sea. Geophys. Res. Lett. 48 (3), e2020GL094545. https://doi.org/10.1029/2021GL09454.